JOINT TRANSMITTER/RECEIVER OPTIMIZATION FOR COGNITIVE RADIO APPLICATIONS

by

Monirosharieh Vameghestahbanati

A Thesis Presented to the Faculty of the
American University of Sharjah
College of Engineering
in Partial Fulfillment of
the Requirements
for the Degree

Master of Science in
Electrical Engineering

Sharjah, United Arab Emirates
May 2012

Acknowledgement

Foremost, I would like to thank Allah for blessing me in my life especially for giving me an insight to select, and to complete this research topic with the best advisors I have ever met, Dr. Hasan Mir and Dr. Mohamed El-Tarhuni. I also would like to thank my parents for their endless love, support, and prayer.

Further, I take this opportunity to express my sincere gratitude to the people who have been conducive in the successful completion of my Master's degree especially Dr. Mohamed Hassan, Dr. Khaled Assaleh, Dr. Maher Bakri, and Dr. Verica Gajic. It is an honor for me to thank the department of Electrical Engineering at the American University of Sharjah for granting me the assistantship package to pursue my Master's degree. My warm thanks also go to all my friends who were supportive in the past two years.

Last but not the least, I would like to offer my greatest appreciation to my thesis advisors who urged my interest in this thesis and enthusiasm to share their outstanding knowledge with me, and for their much appreciated, much patience, much needed, and precious guidance and assistance throughout the thesis. I can't say thank to them enough for their tremendous support and help. I really felt motivated and encouraged every time I attended their meeting. Without their encouragement and guidance this thesis would not have been materialized.

To my lovely parents, brother, and sister

whose love, support, and prayer sustained me throughout

Abstract

The increasing demand for high data rate services is a primary motivation for the development of next generation mobile radio networks. As such, efficient utilization of the available radio spectrum is an important objective to consider. Conventional static frequency allocation schemes are unable to accommodate the increasing number of users. The scarce bandwidth availability thus necessitates some form of spectrum sharing between existing and new users. One such spectrum sharing paradigm is cognitive radio, which offers a highly flexible alternative to the conventional single frequency band wireless devices. Cognitive radio is based on the concept of dynamic spectrum sharing in which the new users use the radio channel only when it is not in use by the primary license-holder user. As such, multiple users may be accommodated within the common frequency band. In this thesis, we examine an alternative paradigm to cognitive radio in which new (overlay) users can operate *simultaneously* with existing (legacy) users. This may potentially unveil an even more efficient utilization of the shared spectrum. However, this mode of operation must contend with mutual interference caused by potentially simultaneous transmissions by the two users. The design of the optimal transmitter and receiver of the overlay system should thus attempt to mitigate the interference received from the legacy user and also the interference caused by the overlay system to the legacy user. A weighted sum of the mean-squared error (MSE) of the overlay system plus the excess MSE in the legacy system due to the introduction of the overlay system is therefore used as a figure of merit. The effects of varying key parameters such as the overlay transmitter power and the amount of channel overlap between the legacy and the overlay systems are investigated. The sensitivity of the system to accuracy of the channel estimate and signal-to-noise ratio (SNR) estimate is also examined. In addition, to reduce the complexity, a system having a fixed transmit-

ter or receiver pulse shape has been studied and the optimum receiver or transmitter for that has been designed, and its performance has been compared with the joint optimization case. Finally, a dual-transmit-antenna overlay system has been proposed and its incurred gain compared to the single-transmit-antenna case has been studied. Simulation results show that using single-transmit-antenna system, 10 dB improvement in the system MSE can generally be achieved by the proposed optimization technique. Additionally, using dual-transmit-antenna system can reduce the system MSE by further 6 dB.

Search Terms—Cognitive radio (CR), mean square error (MSE), crosstalk, overlay system, transmitter/receiver optimization

Table of Contents

List of Figures

List of Tables

List of Abbreviations

AWGN	-	Additive White Gaussian Noise
BER	-	Bit Error Ratio
BPSK	-	Binary Phase Shift Keying
CAF	-	Cyclic Autocorrelation Function
CR	-	Cognitive Radio
CSD	-	Cyclic Spectrum Density
DSSS	-	Direct-Sequence Spread-Spectrum
FCC	-	Federal Communications Commission
FDA	-	Frequency Domain Equalization
FDMA	-	Frequency Division Multiple Acces
FHSS	-	Frequency-Hopping Spread-Spectrum
i.i.d	-	independent and identically distributed
ISM	-	Industrial, Scientific and Medical
MIMO	-	Multiple Input Multiple Output

MISO	-	Multiple Input Single Output
MSE	-	Mean-Squared Error
MMSE	-	Minimum Mean-Squared Error
QoS	-	Quality of Service
ROC	-	Receiver Operating Characteristic
SNR	-	Signal-to-Noise Ratio
TDMA	-	Time Division Multiple Access
VFT	-	Vectorized Fourier Transform

Chapter 1

Introduction

The need for higher data rate communication services has been increasing rapidly due to emerging data and video applications. On the other hand, the available bandwidth does not fulfill the requirements of such high rate data services because of high congestion. Therefore, there should be an efficient spectrum sharing between the legacy (existing) and the overlay (new) systems [1]. In addition, since most of the time the dedicated spectrum to the licensed users (legacy) is underutilized [2], the concept of "dynamic spectrum sharing" has been developed that needs the utilization of cognitive radios to improve the spectrum efficiency [3].

In cognitive radio, the new systems are allowed to occupy the same bandwidth as the already existing ones by sensing the available spectrum and autonomously optimizing their parameters in order not to interfere with the existing users. However, there are many challenges associated with the cognitive radios such as the requirements of sophisticated hardware, the problem of hidden primary user, spectrum sensing in shadowing/fading environments and other problems that will be discussed in further details.

Spectrum sensing is one of the most critical issues in cognitive radios that should be performed in a delicate manner not to disturb the legitimate user and without missing the opportunity to use the vacant spectrum. There are different detection techniques that can be used to sense the presence of the existing user. However, the performance of most of the detectors degrades with channel shadowing or fading. Thus, it is more preferred to use a paradigm which allows the overlay system to operate simultaneously with the legacy

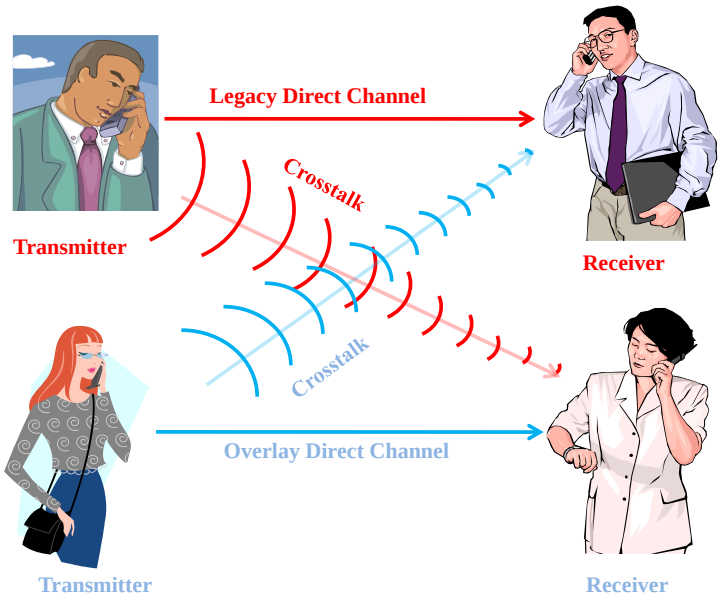

Figure 1.1: Introducing the overlay (secondary) user causes crosstalk to and from the legacy (primary) user.

system rather than an approach that needs continuous spectrum sensing in order to wait for the channel to be empty. Nevertheless, the introduction of the overlay system to the legacy system leads to two kinds of interference: the interference from the legacy system to the overlay system and the interference from the overlay system into the legacy system as shown in Figure 1.1. Additionally, the legacy system already exists with fixed transmitter/receiver response that cannot be modified. Thus, this issue imposes some constraint on the design of the overlay system in order to mitigate interference. To deal with this problem, a figure of merit in terms of the overlay transmitter and receiver can be optimized which unveils more efficient usage of the shared spectrum.

1.1 Objective

The main objective of the present work is to design a cognitive radio framework whereby an overlay system can operate *simultaneously* with a legacy system on a flat Rayleigh fading channel already occupied by a legacy system without the need of sensing the spectrum. Doing so necessitates several things amongst which most importantly it is desired to both

maintain certain level of performance within the overlay system while mitigating any interference or degradation performance due to overlay's operation into the legacy's function.

1.2 Contributions

The main contributions of this thesis are summarized as follows:

1. A wireless system model which tackles the problem of cognitive radio system as the coexistence between the overlay system and the legacy system has been studied.
2. A joint transceiver (transmitter/receiver) optimization for the overlay system has been investigated.
   (a) The sensitivity of the designed transceiver has been studied by comparing its gain with the case when the transmitter and receiver are simply matched filters.
   (b) The effects of varying key parameters such as the overlay transmitter power and the amount of overlap between the legacy and the overlay systems has been addressed.
   (c) The sensitivity of the designed system to accuracy of the channel estimate and the SNR estimate has been examined.
3. A low complexity system with having a fixed transmitter or receiver pulse shape has been studied and the optimum receiver or transmitter for that has been designed, and its performance has been compared with the joint optimization case.
4. A dual-transmit-antenna overlay system has been developed and its incurred gain compared to the single-transmit-antenna case has been studied .

1.3 Thesis Organization

The rest of this thesis is organized as follows. Chapter 2 includes the background behind the CR system along with some literature reviews. Chapter 3 presents the problem formulation

and the methodology used in this research. This chapter also contains the system model for the single-transmit-antenna and the dual-transmit-antenna systems. In Chapter 4, the performance of the designed overlay system from different aspects is assessed via computation examples. Moreover, the sensitivity of the designed overlay system to the accuracy of the channel estimate and the SNR estimate are examined. In addition, the robustness of the system to the transmitter-only optimization the receiver-only optimization is studied. Further, the performance of the dual-transmit-antenna system case is investigated. Chapter 5 concludes this thesis, and also contains some recommendations for the future work.

Chapter 2

Background

This chapter includes an overview to the cognitive radio system along with its different challenges. A review of the current literature is also presented in this chapter.

2.1 Cognitive Radios

The allocation of spectrum space and the issue of the licenses are coordinated by Federal Communications Commission (FCC) in the United States. Recent FCC measurements have indicated that the usage of the licensed frequency bands ranges from 15% to 85% [4]. Efficient spectrum utilization is becoming an important issue, as user demands for data services and data rates increase [3]. Since the natural frequency spectrum is limited, the current static frequency allocation schemes cannot fulfill the requirements of new higher data rate devices. Consequently, it is required to innovate techniques which can offer new ways of exploiting the available spectrum [5].

Cognitive Radios (CR) [6], a low-cost, highly flexible alternate to the classic single frequency wireless devices is considered as a novel approach for improving the utilization of the precious natural frequency spectrum [3][7]. CR is a completely adaptable physical layer whereby sensing the spectrum can autonomously alter its radio features according to the conditions of the wireless channel and to the user's requirement [8]. It is different from traditional radio devices due to its ability to equip users with cognitive capability and reconfigurability. Cognitive capability refers to the ability of the radio to collect or sense the

information from its surroundings. This capability involves identifying the unused portion of the spectrum at a particular time or location. As a result, the cognitive radio device can select the most suitable spectrum and the proper operating parameters. On the other hand, reconfigurability is the ability of the cognitive radio to adjust its operational parameters according to the sensed information in order to attain the best possible performance [2][4].

In cognitive radio terminology *primary* users are wireless devices which possess the main license of the spectrum and have higher priority or legacy rights on the utilization of a particular part of the spectrum. On the contrary, *secondary* users with cognitive capabilities have lower priority on the spectrum and make use of it in such a way that they do not cause interference to primary users. Hence, these cognitive users use their "cognitive" abilities to communicate while ensuring the communication of the primary users is kept at a satisfactory level [5][9].

Cognitive radio functions can be explained through the following cycle of functions [2]:

1. Sensing
2. Analysis
3. Reasoning
4. Adaptation

The CR first performs spectrum sensing and analysis (will be discussed in details in Section 2.4) in order to detect the spectrum white space which refers to as an unused portion of the spectrum.

When the white space has been recognized, the spectrum management and handoff function should be performed to enable the secondary user to choose the best frequency band and to provide it with smooth frequency transition with low latency in case of reappearance of the primary user [2].

Cognitive radio architecture consists of both a secondary and a primary networks. A secondary network consists of a set of secondary users, which can have a secondary base station. The secondary base station has a fixed infrastructure component and coordinates the opportunistic access of the secondary users. Both secondary users and secondary base station have cognitive radio capabilities. A spectrum broker [10] can coordinate the spectrum utilization of several secondary networks sharing one frequency band by collecting operation information from each secondary network.

On the other hand, a set of primary users and one or more primary base stations constitute a primary network that in general does not have cognitive radio capabilities. Hence, in order to avoid interference, the cognitive radio equipped with the secondary network should detect the presence of the primary user on time and direct the transmission of the secondary user to another band.

Cognitive radios are involved on the variety of applications like military communications, commercial markets for wireless technologies, public safety and homeland security enhancement due to their ability to sense, detect and monitor their RF surroundings and to deal with the time varying situations in an autonomous manner [2].

2.2 Spectrum Sensing in Cognitive Radio

Cognitive radios have the lower priority of the spectrum dedicated to the primary user and are considered as the secondary users. So it is required to avoid interference to the primary user in their neighborhood with the constraint of not changing the infrastructure of the primary user network [11]. Hence, the most crucial component for the establishment of the cognitive radio is the task of spectrum sensing which involves the awareness about the utilization of the spectrum and the existence of primary users in a geographical area [5]. Spectrum sensing has various aspects that are discussed below.

2.2.1 challenges.

In this section some of the challenges associated with the spectrum sensing techniques are given.

(a) hardware requirements.

In conventional systems where the receivers are tuned to receive signals transmitted over a limited bandwidth, the noise/interference estimation problem is easier. On the contrary, in cognitive radio, the terminals are required to be capable of processing transmission over a wide band. This will entail radio frequency antennas and power amplifiers. Moreover, cognitive radio imposes the requirements of high speed processing units like DSPs in order to carry out computationally demanding signal processing tasks with fairly low delay.

Single-radio and dual-radio are two different architectures in which sensing can be performed. Single-radio architecture consists of only a specific time slot for spectrum sensing. Thus, the sensing duration is limited and has poor spectrum accuracy. In addition, using some portion of the available time slot for sensing instead of data transmission will degrade the spectrum efficiency. However, it is simple and has low cost. Conversely, dual-radio sensing architecture consists of two radio chains: one for data transmission and reception and the other one for spectrum monitoring. This sensing architecture provides higher spectrum efficiency and better sensing accuracy but at the expense of higher cost, more power consumption, and higher complexity.

(b) hidden primary user problem.

Sometimes, in the presence of severe multipath fading or shadowing the primary user is hidden to the secondary one and cannot be detected. This will introduce unwanted interference to the primary user. Cooperative sensing which will be elaborated later is used to overcome this problem [5].

(c) detecting spread spectrum primary users.

Fixed frequency and spread spectrum are two core types of technologies for commercially available devices where frequency-hopping spread-spectrum (FHSS) and direct-sequence spread-spectrum (DSSS) are the two main spread spectrum schemes. Fixed frequency devices function at a single frequency while the FHSS devices perform frequency hopping to change their operational frequencies dynamically to multiple narrowband channels according to a known sequence. Also, DSSS devices use a single band to spread their energies. Since in spread spectrum devices the power of the primary user is distributed over a wide range of frequency, they are difficult to be detected. However, by knowing the hopping pattern and performing perfect synchronization to the signal this problem can be partly solved.

(d) sensing duration and frequency.

As mentioned earlier, the primary user has the priority to use the frequency band and can claim it at any time. Thus, cognitive radio should be capable of identifying the presence of the primary user within specific time interval in order to avoid interference. Therefore, one of the design parameter that needs to be selected cautiously is the sensing frequency which is defined as how frequently cognitive radio should carry out spectrum sensing.

(e) security.

In cognitive radio, an egotistic user can mislead the spectrum sensing performed by legitimate primary users by modifying its air interface to imitate a primary user. To handle this problem, an encrypted value is transmitted by the legal primary users to be used for validating them. However, this requires coordination and synchronization between the primary and the secondary users.

2.2.2 multi-dimensional spectrum sensing.

Spectrum sensing can be performed in multi-dimensions in order to improve the spectrum efficiency. The multi-dimensional radio spectrum sensing and the transmission opportunities are given below [5].

(a) frequency dimension.

The frequency dimension involves sensing the frequency and opportunity in the frequency domain. As the available spectrum is divided into narrower chunks, some of the band may be available.

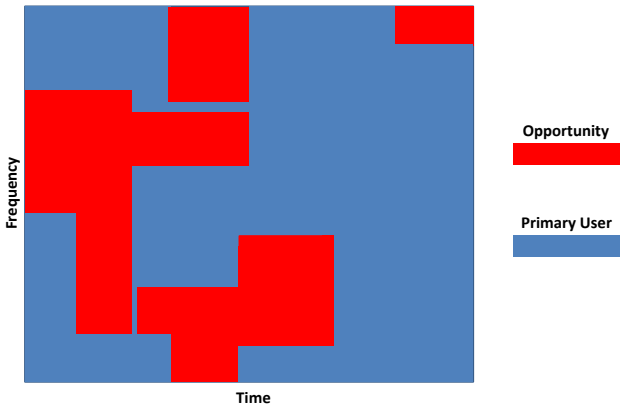

(a)

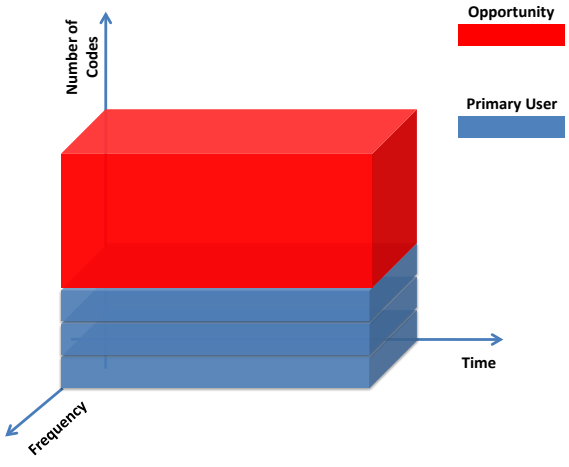

(b)

Figure 2.1: Illustration of (a)frequency and time dimensions. (b)code dimension.

(b) time dimension.

Since the band is not continuously in used, some specific part of the spectrum might be available in time and provide an opportunity for the secondary user. The frequency and time dimensions are illustrated in Figure 2.1(a).

(c) code dimension.

By transmitting an orthogonal code with respect to codes that is used by the primary user, simultaneous transmission without interference with the primary user can be achievable. This requires timing information for the secondary user to synchronize itself with the primary user that uses time hopping or frequency hopping. Figure 2.1(b) illustrates the code dimension.

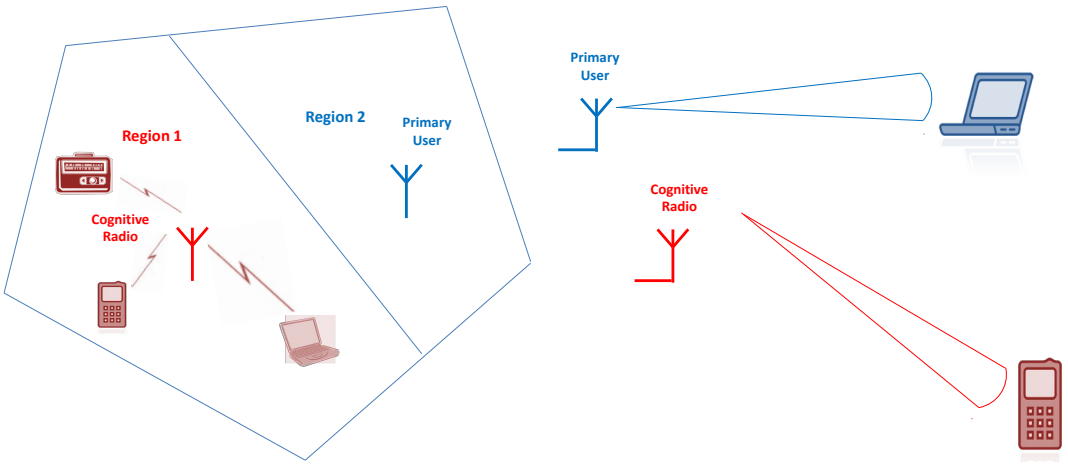

(a) (b)

Figure 2.2: Illustration of (a)geographical space dimension. (b)angle dimension.

(d) geographical space dimension.

Since in a given time the spectrum can be accessible in some parts of the geographical area while it is unavailable in some other parts, the geographical space can be consider as one dimension. This means the location i.e. its latitude, longitude, elevation, and the distance of the primary users should be sensed. This dimension is illustrated in Figure 2.2(a).

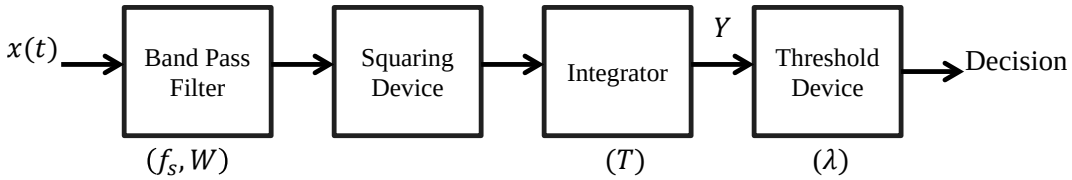

Figure 2.3: Block diagram of an energy detector.

(e) angle dimension.

The latest progresses in multi-antenna technologies allow multiple users to be multiplexed into the same channel at the same time in the same environmental area. Thus, by sensing the direction of the primary user beam i.e. the azimuth and the elevation angle and the location of the primary user, the secondary user can transmit in other directions without interfering with the primary one. The illustration of the angle dimension is given in Figure 2.2(b).

2.2.3 spectrum sensing methods.

In this section, some of the main spectrum sensing techniques are presented.

(a) energy detector-based sensing.

In cognitive radio, to detect the unknown signals in the presence of noise, energy detection based sensing is commonly used. In Figure 2.3, the block diagram of an energy detector is depicted. The center frequency, f_s, and the bandwidth of interest will be selected by the input band pass filter. Then, the received energy signal will be measured by a squaring device which is followed by an integrator to determine the observation interval, T. Afterward, the output of the integrator, Y, will be compared with a threshold, λ, to identify the presence of the signal [12].

This approach is simple to implement and does not require preceding acquaintance about the primary signal as the threshold, λ, depends on the noise floor. On the other hand, the choice of the threshold is not easy and this method will fail in the low signal-to-noise ratio scenarios, because it is not capable of differentiating between the interference from the primary users and noise [2][5].

The performance of the energy detector based sensing in fading channels will be discussed in Section 2.5.

(b) waveform-based sensing.

In wireless systems, known patterns are usually used to aid synchronization or for other purposes. For example, a preamble is a recognized sequence transmitted before each burst or slot while a midamble is transmitted in the middle of it. If the pattern is known, by correlating the received signal with a known copy of itself sensing can be done. Hence, the waveform-based sensing can be only applied to systems having known signal patterns. This method is more reliable compared to energy detector based sensing. Assuming that the received signal has the following form

$$y(k) = s(k) + w(k), \tag{2.1}$$

where $s(k)$ is the kth sample primary signal which should be detected, $w(k)$ is the additive white Gaussian noise (AWGN) sample, and k is the index of the sample. If the known time-domain signal pattern has K signal samples, the decision metric for the waveform based sensing can be written as [13]

$$M = \mathcal{R}e\left[\sum_{k=1}^{K} y(k)s^*(k)\right], \tag{2.2}$$

where $()^*$ is the complex conjugation operation. When the primary user is absent, the metric is

$$M = \mathcal{R}e\left[\sum_{k=1}^{K} w(k)s^*(k)\right] \tag{2.3}$$

When the primary user is present, the metric becomes

$$M = \sum_{k=1}^{K} |s(k)|^2 + \mathcal{R}e\left[\sum_{k=1}^{K} w(k)s^*(k)\right] \tag{2.4}$$

By comparing the decision metric M with a fixed threshold λ_w, the decision will be made [5]. In other words, if the value of M exceeds the value of threshold the spectrum is busy, otherwise it is empty.

(c) cyclostationarity-based sensing.

By exploiting the cyclostationarity features of the received signals, the primary user can be detected. This method is called cyclostationary feature detection. Cyclostationary features concerns with the periodicity in the signal or in its statistics like its mean or its autocorrelation.

One of the main advantages of the cyclostationary-based sensing is its ability to discriminate noise from primary users' signals. This is because noise is wide sense stationary and has no periodicity in its correlation function, while the modulated signal is cyclostationary with spectral correlation [5].

Unlike the energy-based detector with having time-domain signal energy as its test statistics, Cyclostationarity- Based Sensing conducts a hypothesis test in the frequency domain. The hypothesis model of the received signal can be assumed as [2]

$$\begin{aligned} \mathcal{H}_0 &: y(k) = w(k), \\ \mathcal{H}_1 &: y(t) = hs(k) + w(k), \end{aligned} \tag{2.5}$$

where h is the channel gain from the transmitter of the primary user to the receiver of the secondary one. $\mathcal{H}_0$ is the null hypothesis indicating the absence of the primary user in the band of interest while $\mathcal{H}_1$ indicates the presence of the primary user. The cyclic autocorrelation function (CAF) of the received signal is defined as

$$R_y^{\alpha}(\tau) = E\left[y\left(k+\tau\right) y^*\left(k-\tau\right) e^{j2\pi\alpha k}\right] \tag{2.6}$$

$E[.]$ is the expectation and α is the cyclic frequency. Since the digitally modulated signal is periodic, the CAF of the received signal is also periodic. By applying the Fourier series

expansion to (2.6), the cyclic spectrum density (CSD) function, can expressed as

$$S\left(f,\alpha\right)=\sum_{\tau=-\infty}^{\infty}R_{y}^{\alpha}(\tau)e^{-j2\pi f\tau}, \tag{2.7}$$

When the cyclic frequency α equals to the fundamental frequency of the transmitted signal $s(k)$, the CSD function will output its peak values. However, the CSD has no peaks under the $\mathcal{H}_0$ hypothesis, since the noise is not cyclostationary signal. Consequently, a peak detector can be used to differentiate the two hypotheses.

(d) matched filtering.

The optimal detector in stationary Gaussian noise is a matched-filter with a threshold test when the primary signal is known to the secondary user. On the contrary, it is difficult to implement such a detector [12] because the secondary user requires perfect knowledge of the primary user's signal such as bandwidth, operating frequency, modulation type, channel, etc [5].

2.2.4 cooperative spectrum sensing.

Noise, shadowing, and multi-path fading are the three most important factors that limit the performance of the spectrum sensing. When the received SNR of the primary signal is too low, even with long sensing time, reliable spectrum sensing is very difficult. As a result, the primary user cannot be detected and will experience unwanted interference. To overcome this problem, cooperative spectrum sensing, which uses control channel in order to share the results of spectrum sensing and channel allocation information, has been introduced.

Cooperation increases the probability of detection in order to better protect the primary signal and decreases the false alarm in order to use the vacant spectrum in an efficient manner [2]. It also can solve the hidden primary user problem (discussed in Section 2.2.1) and can decrease sensing time [5].

On the other hand, there are some challenges associated with the cooperative sensing. For example, when the cooperative sensing is wide band, multiple secondary users

have to inspect a wide range of spectrum channels which results in a large amount of data exchange, high consumption of energy and a lower data throughput [2].
Three main categories of cooperative sensing are discussed below:

(a) centralized sensing.

There exists a central entity which collects sensing information from cognitive devices and identifies the available spectrum. The central unit broadcasts this information to other cognitive radios or it can directly control the cognitive radio traffic. The required bandwidth for reporting the information becomes huge in case of large number of users. To reduce the sharing bandwidth, only cognitive radios with consistence information can report their decisions to the central unit. Thus, censoring some sensors is required.

(b) distributed sensing.

If the cognitive nodes can share information among each other but can make their own decisions about the part of the spectrum they can use, spectrum sensing is in a distributed manner. Unlike the centralized sensing, distributed sensing does not require a backbone infrastructure and thus, has less cost. However, collaboration can increase the network overhead that is overcome by sharing only the final decisions.

(c) external sensing.

In external sensing, the sensing is performed by an external agent, which broadcasts the channel occupancy information to the cognitive radios. Handling the hidden primary user problem and the uncertainty due to shadowing and fading are the two main advantages of the external sensing. In addition, external sensing increases the spectrum efficiency since the cognitive radios do not spend time for sensing. Moreover, it has less power consumption compared to internal sensing, as the sensing network does not need to be mobile and not necessarily powered by batteries [5]. On the other hand, the control channel between the secondary user and the sensing device can get congested for a large secondary network with a large number of users [14].

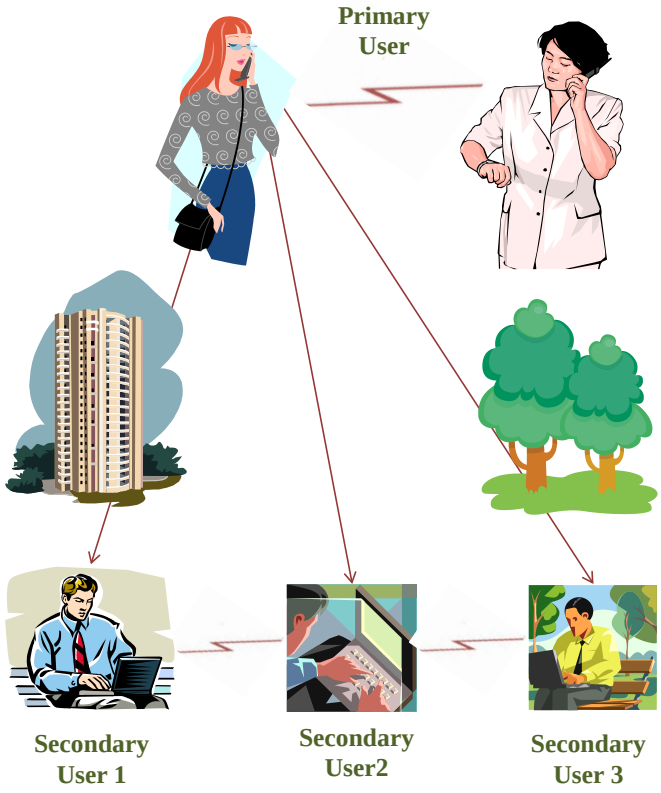

Figure 2.4: Cooperative spectrum sensing in a shadowed environment.

2.3 Performance Metrics in Cognitive Radio

As mentioned earlier, cooperative technique can be used in order to improve spectrum sensing. As shown in Figure 2.4, deep shadowing effect does not allow some of the secondary users to sense the present primary user and only few of them may be able to detect the primary signal. Hence, to improve the secondary spectrum access cooperation can be used. This section concerns with the performance of local and cooperative sensing of an energy detector-based sensing in fading channels [12].

The purpose of spectrum sensing is to distinguish between the two hypotheses given in (2.5). In a non-fading environment, h is deterministic and the detection and false alarm probabilities are given by the following formulas,

$$P_d = P\{Y > \lambda \,|\mathcal{H}_1\} \tag{2.8}$$

$$P_f = P\{Y > \lambda \,|\mathcal{H}_0\} \tag{2.9}$$

where Y is the output of the integrator in Figure 2.3.

In the context of dynamic spectrum sharing, there should be a fundamental tradeoff between $P_m = 1 - P_d$ (probability of missed detection) and P_f. If P_m is high, the presence of the primary user will be missed with high probability which results in introducing undesired interference to it. On the contrary, if P_f is high, number of missed opportunities will be increased which in turn leads to low spectrum utilization.

Because under $\mathcal{H}_0$ there is no primary signal, the false alarm probability is independent of signal to noise ratio (γ). In contrast, (2.8) gives the detection probability conditioned on the instantaneous SNR, γ when h is varying due to shadowing or fading.

In [12], the performance of an energy detector-based sensing under Rayleigh fading with AWGN case is shown to suffer significant degradation compared to the case without fading. In particular, to achieve $P_m < 10^{-2}$ involves the false alarm probability greater than 0.9 which will result in poor spectrum usage.

By allowing different secondary users to cooperate by sharing their information, the performance of spectrum sensing improves considerably.

Let l be the number of cooperative users. Also, assume that fading for all users is independent and identically distributed (iid). Then, the detection and false alarm probabilities for the cooperative scheme (Q_d and Q_f) can be written as,

$$Q_d = 1 - (1 - P_d)^l \tag{2.10}$$

$$Q_f = 1 - (1 - P_f)^l \tag{2.11}$$

where P_d and P_f are defined by (2.8) and (2.9) respectively. It is obvious from (2.10) and (2.11) that cooperative scheme increases detection and false alarm probabilities.

A typical presentation of the detector performance is through the complementary receiver operating characteristic (ROC) curve (plot of P_m versus P_f) for different number of cooperative users. It is shown in [12] that cooperative sensing significantly improves the

performance of an energy-based detector. In addition, as l increases, the performance will be even better than AWGN case with $l = 1$.

2.4 Dynamic Spectrum Allocation and Sharing

In the previous section, the various aspects of the spectrum sensing have been discussed. It is important to note that the primary users' activity and competition from other secondary users may change the availability and quality of a frequency band. Thus, the secondary user has to be able to perform dynamic spectrum allocation and sharing. The existing spectrum allocation and sharing schemes are classified in to two categories: open spectrum sharing, and hierarchical access (licensed spectrum sharing).

In open spectrum sharing, the secondary user can only access the unlicensed frequency bands such as the unlicensed industrial, scientific, and medical (ISM) band. The secondary users can simultaneously transmit with primary users subject to interference constraints. They have a centralized network architecture in which a central unit controls the allocation and the access of the spectrum. All secondary users have same rights in using the unlicensed spectrum.

In a hierarchical access model, the secondary users can also access the licensed spectrum band and are able to use the licensed spectrum, only when the primary user is absent. Hence, they must have cognitive radio capabilities to detect the presence of the primary user and to vacate the band immediately in order not to interfere with the primary user. Additionally, they have distributed network architecture in which each user can make his/her own decision on the access of the spectrum [2].

There exist three types of cognitive behavior in a licensed spectrum: Interference avoiding behavior (spectrum interweave), Interference controlling behavior (spectrum underlay), and Interference mitigating behavior (spectrum overlay).

In an interference avoiding behavior, the secondary user occupies the primary user's band without introducing any interference to it as if its signal is orthogonal to the primary one. The primary and secondary users may access the spectrum in a fashion that ensures

no interference between them like time-division-multiple-access (TDMA) or frequency-division-multiple-access (FDMA). As a result, the secondary user should have the knowledge of the white spaces in order not to lose any opportunities.

In an interference controlling behavior, the secondary and the primary users can concurrently transmit in the same spectrum with primary user's interference constraint. It is called spectrum underlay since the cognitive radio signal appears as noise under the primary signal [9].

Traditionally, by limiting the power of the interfering user, the interference level of the primary user is kept below an acceptable level. On the contrary, as unpredictable new sources of interference may appear, constraining the transmitter power becomes more challenging. Thus, FCC Spectrum Policy Task Force has proposed metric on interference judgment called *interference temperature*, which imposes an interference limit perceived by receivers. Interference temperature is defined as *"the temperature equivalent to the RF power available at a receiving antenna per unit bandwidth"* [2], which is

$$T_I\left(f_c, B\right) = \frac{P_I\left(f_c, B\right)}{KB} \tag{2.12}$$

Where, $P_I\left(f_c, B\right)$ is the average interference power measured in Watt centered at f_c with bandwidth B that is measured in Hertz and K is the Boltzmann's constant $(K = 1.38 * 10^{-23})$ Joules per degree Kelvin.

For an unlicensed secondary user using the same band as the primary user to co-exist with it, its transmission plus the existing noise and interference must not exceed the interference temperature limit at a licensed receiver. For instance, if a licensee user has an interference temperature limit T_L for a specific spectrum with bandwidth B, in that case the secondary transmitter has to maintain the average interference below KBT_L.

In an interference mitigating behavior, the secondary user can occupy the same spectrum as the primary user by knowing its channel with the primary user along with some additional information about the primary system's operation. For instance, it should have some knowledge about the primary user's codebook in order to decode the primary

user's transmission or sometimes it should have some information about the primary user's message [9].

2.5 Cognitive Radio Channel Model

As mentioned earlier, identifying other radios in the environment that use the same spectral resources in order to design a transmission policy that mitigates interference to and from those radios is the major value of a CR system. The system designer can determine the transmitted power from the secondary transmitter, however, the amount of the transmitted power that will be arrived at the secondary receiver, and also the amount of interference that is created at the primary receiver is determined by the channel. Therefore, it is essential to understand the channel for the design and analysis of the transmission policy [15].

There are variety of channel models each of which are appropriate for certain scenarios or environmental condition. However, in this work we will be assuming a standard Rayleigh fading model that is also consistent with other work in the literature such as [16]–[22].

2.6 Optimum System Design for Mutual Interference Mitigation

In this research, we employ joint trasmitter/receiver optimization using an MSE (mean-squared error) based criterion, to design an overlay system for cognitive radio application. This CR system allows the legacy *and* the overlay users to simultaneously share the spectrum under the constraint that the overlay user does not cause significant degradation in the performance of the legacy system.

Joint transmitter/receiver optimization under the MSE criterion has been widely studied in wireless and wireline communications e.g [1], [23]–[28]. [1] and [23] consider the introduction of an overlay system to a legacy system in a non-coordinated digital subscriber line. The performance metric in [1] consists of the overlay system MSE and the excess MSE to the legacy system caused by the introduction of the overlay system, while

[23] uses a composite MSE of convex form consisting of a weighted sum of the MSE of the overlay system and the excess MSE in the legacy system as a figure of merit.

An iterative optimization method of transmit/receive frequency domain equalization (FDE) was proposed in [24] for single carrier transmission systems, where a recursive algorithm is used to determine the transmit and receive FDE weights iteratively in order to minimize the error signal at a virtual receiver.

A joint transmitter/receiver optimization for multiple uncoordinated users in a communication system assuming that both the direct and cross talk channel responses seen by each user are symmetric is investigated in [25]. In [26], a joint optimization of transmitter and receiver that minimizes the MSE of the output receiver under an average transmitter power constraint is proposed using vectorized Fourier transform (VFT). [27] solved the joint transmitter/receiver optimization problem of [26] in a more constrained manner such that the overlay system introduces zero interference to the legacy system(s) already existing in the desired frequency band. Using VFT, [28] addressed the design of an overlay system in a wide-sense cyclostationary legacy signal by minimizing the output MSE of the overlay receiver subject to inducing no interference to the legacy system. It is assumed that the channel from the overlay transmitter to the overlay receiver is slowly time-varying relative to the transmission rate.

In [29], a joint transmitter and receiver optimization scheme for a spatial multiplexing system in a narrowband wireless channel is proposed. It is shown that the multiple input multiple output (MIMO) channels are decoupled into parallel sub-channels by the transmit and receive filters, which perform a form of inverse water-filling on the eigen-modes of the MIMO channel. [30] considers the design problem of linear minimum MSE transceiver for downlink multiuser MIMO systems where imperfect channel state information is available at the base station and mobile stations. [31]-[32] formulates the sum MSE as a convex optimization problem in which global optimal solution can be efficiently obtained in an uplink channel for a MIMO system.

In the context of cognitive radio network, [33] proposed a robust MSE-based transceiver optimization in multiple input-single output (MISO) cognitive radio network, while [34]

proposed a robust MSE-based transceiver optimization in MIMO CR system where both the new and the overlay systems can share the same spectrum band. [35] studied the problem of joint precoder and receiver using MSE criterion between the transmitted signal of the new system and its estimate in the receiver for downlink single-user MIMO system. [36] presented a framework to solve the spectrum sharing problem in cognitive wireless network by considering both interference constraints for the legacy users and quality of service (QoS) constraints for the overlay users.

In this work, we investigate the impact of joint transmitter/receiver pulse shape optimization for improved crosstalk cancellation in wireless co-channel systems with single transmit antenna or dual transmit antennas under the constraint that the legacy system has a fixed infrastructure that cannot be further modified. Although the bit error ratio (BER) may be a more appropriate performance measure of communication systems quality, it is not analytically tractable. However, the MSE is related to the BER; As such, the figure of merit used in this work consists of the MSE into the overlay system and the excess MSE introduced into the legacy system. Part of the results of this research is presented in [37].

Chapter 3

Proposed Overlay Cognitive Radio System

In this chapter, the problem formulation and the methodology used in this research are presented. This chapter also contains the system model for the single-transmit-antenna and the dual-transmit-antenna systems.

3.1 Single-Transmit-Antenna System

As mentioned before, one of the main objectives of the present work is to explore a method to allow the secondary users to work simultaneously with the primary ones without the need of vacating the channel. This can be done by optimizing the transmitter and the receiver filters of the secondary users to optimize self- performance and mitigate interference to the primary users. To design the desired transmitter-receiver filter the MSE of the overlay system plus the excess MSE in the legacy system is used as the figure of merit which is shown in Figure 3.1.

3.1.1 system model.

The system model is given in Figure 3.2 where the upper branch represents the legacy system with fixed transmitter and receiver filters with impulse responses $h_t^{(l)}(t)$ and $h_r^{(l)}(t)$, respectively, while the lower branch represents the overlay system with transmitter and receiver filters with impulse responses $h_t^{(o)}(t)$ and $h_r^{(o)}(t)$, respectively. The legacy system operates over the channel with impulse response $h_c^{(ll)}(t)$ while the overlay system

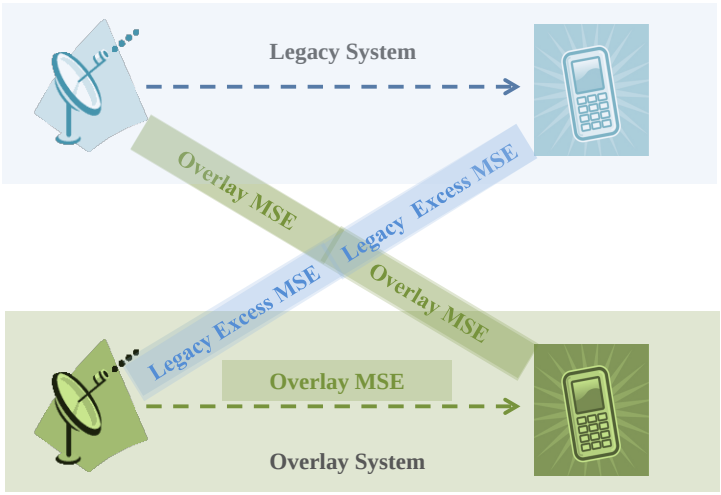

Figure 3.1: Overlay MSE and legacy excess MSE.

works over the channel $h_c^{(oo)}(t)$. As shown in the figure, $h_c^{(ol)}(t)$ and $h_c^{(lo)}(t)$ represent the crosstalk (interference) between the two systems. The input signals to the overlay and legacy receivers are corrupted by AWGN sequences $w_1(t)$ and $w_2(t)$, respectively.

Our objective is to design a wireless system whereby an overlay system can operate *simultaneously* with a legacy system without waiting for the channel to be vacant by jointly optimizing the overlay transmitter $h_t^{(o)}(t)$ and receiver $h_r^{(o)}(t)$, while simultaneously mitigating interference to the legacy system subject to the constraint that the legacy system has a fixed impulse response. A composite MSE which considers the performance of the new system and the performance degradation of the existing one due to the introduction of the overlay system, is used as a figure of merit. It is assumed that the both systems occupying the same bandwidth. Channel knowledge is assumed to be available via estimation, so that $h_c^{(oo)}(t)$, $h_c^{(ll)}(t)$, $h_c^{(ol)}(t)$, and $h_c^{(lo)}(t)$ are known a priori. This assumption will be relaxed later on as we present the sensitivity of the performance to channel estimation error.

3.1.2 problem formulation.

In Figure 3.2, we assume that the legacy system has independent and identically distributed (i.i.d) input sequence $z_{2n} \in \{\pm 1\}$. This signal is input to the legacy transmitter with a fixed impulse response $h_t^{(l)}(t)$, which then transmits the message over the legacy channel

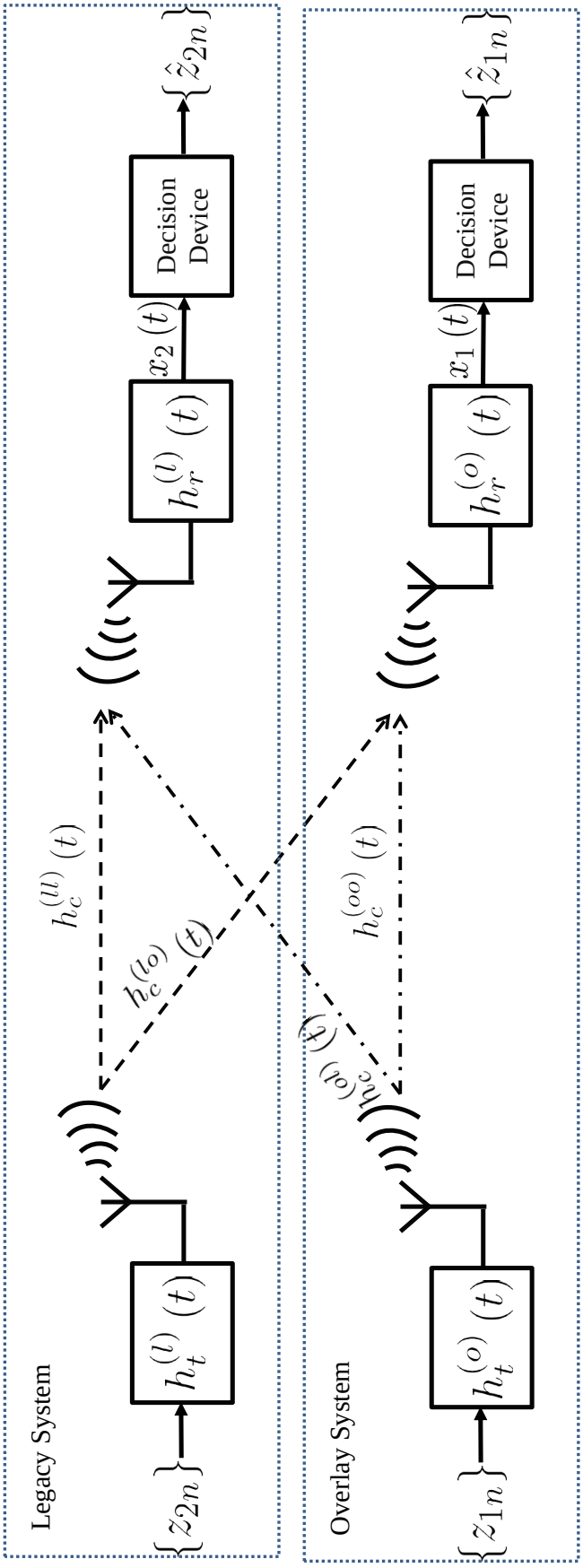

Figure 3.2: Single-transmit-antenna system model.

$h_c^{(ll)}(t)$. The AWGN, $w_2(t)$, is added to the message at the input receiver. The message is then picked up by the legacy receiver with a fixed impulse response, $h_r^{(l)}(t)$. The output of the legacy receiver $x_2(t)$, is processed by the decision device to produce the final estimate $\hat{z}_{2n}$. In the lower branch of the system, the i.i.d sequence $z_{1n} \in \{\pm 1\}$ of the overlay system is processed by the overlay transmitter filter with impulse responses $h_t^{(o)}(t)$ that we wish to design. $h_c^{(oo)}(t)$ represents the overlay channel impulse response and $w_1(t)$ is additive white Gaussian noise added to the signal at the input of the overlay receiver. It is assumed that z_{1n}, z_{2n}, $w_1(t)$, and $w_2(t)$ are mutually independent. The signal is then processed by the overlay receiver filter with impulse response $h_r^{(o)}(t)$, which we also aim to design, to produce an output $x_1(t)$ that is the input to the decision device to make the final estimate $\hat{z}_{1n}$. $h_c^{(lo)}(t)$ and $h_c^{(ol)}(t)$ represent the crosstalk channel between the two systems.

In this research, we assume that the channels between the transmitter/receiver of both systems, $h_c^{(oo)}(t)$, $h_c^{(ll)}(t)$, $h_c^{(ol)}(t)$, and $h_c^{(lo)}(t)$, follow a complex Gaussian distributions which lead to Rayleigh fading channels representing the mobile wireless systems.

Given the constraint that the legacy system is fixed and cannot be modified, a composite MSE is given by

$$MSE = MSE_1 + \beta MSE_2^e \tag{3.1}$$

where

$$\begin{aligned} MSE_1 &\equiv \text{MSE in channel 1 (overlay MSE)} \\ &= E\left[|z_{1n} - \hat{z}_{1n}|^2\right] \end{aligned} \tag{3.2}$$

$$\begin{aligned} MSE_2^e &= \text{legacy excess MSE} \\ &= E\left[|q_{2n}|^2\right] \end{aligned} \tag{3.3}$$

and

$$q_{2n} \triangleq q_2(t)\Big|_{t=nT} \tag{3.4}$$

$$q_2(t) = h_t^{(o)}(t) * h_c^{(ol)}(t) * h_r^{(l)}(t) \tag{3.5}$$

where $*$ denotes the convolution and MSE_2^e in (3.3) represents the excess MSE into the legacy system due to the interference from the overlay system. The constant β is a weighting in the optimization problem between MSE_1 and MSE_2^e and can be selected to weight or de-weight MSE_2^e by using large value or small value of β, respectively.

The output signals $x_1(t)$ and $x_2(t)$ are produced by processing the signal at the receiver input in the presence of AWGN $w_1(t)$ and $w_2(t)$ through the receiver filters $h_r^{(o)}(t)$ and $h_r^{(l)}(t)$ and are the input to the decision device (which is actually a sampler followed by a threshold comparison) to generate the final estimates,

$$\begin{aligned} x_1(t) &= \sum_{n=-\infty}^{\infty} z_{1n} p_{11}(t - nT) \\ &\quad + \sum_{n=-\infty}^{\infty} z_{2n} p_{21}(t - nT) + \upsilon_1(t) \end{aligned} \tag{3.6}$$

$$\upsilon_1(t) = w_1(t) * h_r^{(o)}(t) \tag{3.7}$$

$$S_{\upsilon_1} = N_0 \left| H_r^{(o)}(f) \right|^2 \tag{3.8}$$

where S_{υ_1} denotes the power spectral density of $\upsilon_1(t)$, N_0 is the additive noise power spectral density, and

$$p_{11}(t) = h_t^{(o)}(t) * h_c^{(oo)}(t) * h_r^{(o)}(t) \tag{3.9}$$

$$p_{21}(t) = h_t^{(l)}(t) * h_c^{(lo)}(t) * h_r^{(o)}(t) \tag{3.10}$$

$H_r^{(o)}(f)$ in (3.8) represents the Fourier transform of the pulse shape of the overlay receiver $h_r^{(o)}(t)$, and similar notations are used for the transmitter and channel as shown in Table 3.1.

It is assumed that both the overlay and the legacy systems have the same bandwidth $1/T$, where T denotes the symbol period.

Table 3.1: Notations for Fourier transform pair

$h_t^{(l)}(t)$	$\leftrightarrow$	$H_t^{(l)}(f)$
$h_t^{(o)}(t)$	$\leftrightarrow$	$H_t^{(o)}(f)$
$h_c^{(ll)}(t)$	$\leftrightarrow$	$H_c^{(ll)}(f)$
$h_c^{(oo)}(t)$	$\leftrightarrow$	$H_c^{(oo)}(f)$
$h_c^{(lo)}(t)$	$\leftrightarrow$	$H_c^{(lo)}(f)$
$h_c^{(ol)}(t)$	$\leftrightarrow$	$H_c^{(ol)}(f)$
$h_r^{(l)}(t)$	$\leftrightarrow$	$H_r^{(l)}(f)$
$h_r^{(o)}(t)$	$\leftrightarrow$	$H_r^{(o)}(f)$

3.1.3 optimal mmse solution for single-transmit-antenna overlay system design.

It is assumed that $x_1(t)$ is synchronously sampled at instants nT; the sample at instant $t = m$ is represented by x_{1m} and σ^2 denotes the input symbol variance. Note the assumption $z_{1n} \in \{\pm 1\}$ implies $\sigma^2 = 1$. Then, as shown in Appendix A.1 the overlay MSE (MSE_1) is given by

$$\begin{aligned} E\left[|x_{1m} - z_{1m}|^2\right] &= \frac{\sigma^2}{T}\int_{-\frac{1}{2T}}^{\frac{1}{2T}} \left|H_t^{(o)}(f)\, H_c^{(oo)}(f)\, H_r^{(o)}(f) - T\right|^2 df \\ &\quad + \frac{\sigma^2}{T}\int_{-\frac{1}{2T}}^{\frac{1}{2T}} \left|H_t^{(l)}(f)\, H_c^{(lo)}(f)\, H_r^{(o)}(f)\right|^2 df \\ &\quad + N_0 \int_{-\frac{1}{2T}}^{\frac{1}{2T}} \left|H_r^{(o)}(f)\right|^2 df \end{aligned} \tag{3.11}$$

The first term in (3.11) is related to the overlay system itself and is a constant number; the second term denotes the interference from the legacy system to the overlay system and the last term is referred to the noise power. The legacy excess MSE is given as

$$MSE_2^e = \frac{\sigma^2}{T}\int_{-\frac{1}{2T}}^{\frac{1}{2T}} \left|H_t^{(o)}(f)\, H_c^{(ol)}(f)\, H_r^{(l)}(f)\right|^2 df \tag{3.12}$$

The average transmitter power on the overlay user is

$$P_t = \frac{\sigma^2}{T} \int_{-\frac{1}{2T}}^{\frac{1}{2T}} \left| H_t^{(o)}(f) \right|^2 df \tag{3.13}$$

The optimization problem is to minimized (3.1) subject to the average power constraint in (3.13) can be rewritten as below by introducing a Lagrange multiplier λ

$$MSE = MSE_1 + \beta MSE_2^e + \lambda P_t \tag{3.14}$$

where λ in (3.14) is increased if the overlay transmitter power is too high in order to be emphasized in the optimization. On the other hand, if the overlay transmitter power is too low, λ is decreased in order to be de-emphasized.

We consider the case in which both systems are confined to a bandwidth of $1/T$ (one Nyquist zone). By solving (3.14) and noting that,

$$\left| H_t^{(o)}(f) \right|^2 = G \left| H_r^{(o)}(f) \right|^2 \tag{3.15}$$

where

$$G = \frac{\left| H_t^{(l)}(f) \right|^2 \left| H_c^{(lo)}(f) \right|^2 + \eta^{-1}}{\beta \left| H_r^{(l)}(f) \right|^2 \left| H_c^{(ol)}(f) \right|^2 + \lambda} \tag{3.16}$$

and

$$\eta = \frac{\sigma^2}{N_0 T} \tag{3.17}$$

as shown in Appendix A.1, the following equation is obtained

$$a|H_r^{(o)}(f)|^4 + b|H_r^{(o)}(f)|^2 + c = 0 \tag{3.18}$$

where

$$a = G|H_c^{(oo)}(f)|^4 \tag{3.19}$$

$$b = |H_c^{(oo)}(f)|^2 \left[|H_t^{(l)}(f)|^2 |H_c^{(lo)}(f)|^2 + \eta^{-1} + (\beta |H_r^{(l)}(f)|^2 |H_c^{(ol)}(f)|^2 + \lambda) G \right] \tag{3.20}$$

and

$$c = \left[\beta |H_c^{(ol)}(f)|^2 |H_r^{(l)}(f)|^2 + \lambda\right] \left[|H_t^{(l)}(f)|^2 |H_c^{(lo)}(f)|^2 + \eta^{-1}\right] - T^2 |H_c^{(oo)}(f)|^2 \quad (3.21)$$

It is clear that (3.18) is a quadratic function in $|H_r^{(o)}(f)|^2$; thus, by solving for the roots of (3.18) and substituting for $|H_r^{(o)}(f)|^2$ in (3.15) the optimal transmitter can be obtained, as indicated in the pseudo code in Algorithm 1.

Algorithm 1 Single-transmit-antenna program pseudo code

```
Choose an initial value for λ.
Select desired transmitter power level P.
Select tolerance power level δ (typically δ = 0.1 dB)
for f_n ∈ [−1/2T,1/2T] do
    while |P_t − P| > δ do
        Compute optimal receiver from (3.18).
        Compute optimal transmitter from (3.15).
        Compute transmitter power (P_t) from (3.13).
        if P_t > P then
            Increase λ.
        else
            Decrease λ.
        end if
    end while
    Compute the optimum MSE from (3.14).
end for
```

To model the inaccuracy in estimating the channels, we assume that these channels are subject to random errors each following a complex Gaussian distribution with zero mean and a variance of σ_i^2, $i = 1, 2, 3$ that could be different for different channels; i.e.

$$\hat{h}_c^{(oo)}(t) = h_c^{(oo)}(t) + \mathcal{CN}\left(0, \sigma_1^2\right)$$

$$\hat{h}_c^{(ol)}(t) = h_c^{(ol)}(t) + \mathcal{CN}\left(0, \sigma_2^2\right)$$

$$\hat{h}_c^{(lo)}(t) = h_c^{(lo)}(t) + \mathcal{CN}\left(0, \sigma_3^2\right) \quad (3.22)$$

The perturbation variance to each channel is modeled as follows in order to reflect the

inexactness of the estimation error that corresponds to the nature of each channel

$$\begin{aligned} \sigma_1^2 &= k\sigma_{oo}^2 \\ \sigma_2^2 &= k\sigma_{ol}^2 \\ \sigma_3^2 &= k\sigma_{lo}^2 \end{aligned} \tag{3.23}$$

where σ_{oo}^2 is the variance of $h_c^{(oo)}$, σ_{ol}^2 is the variance of $h_c^{(ol)}$, σ_{lo}^2 is the variance of $h_c^{(lo)}$, k is ratio between the perturbation variance and the actual channel variance, and $0 \leq k \leq 1$.

3.2 Dual-Transmit-Antenna System

The use of MIMO systems can improve the spectral efficiency of wireless channels by exploiting the transmit and receive diversity [30]. In this section, we introduce a dual-transmit-antenna overlay system which leads to more efficient usage of spectrum.

3.2.1 system model.

The system model is given in Figure 3.3 where the upper branch represents the legacy system with fixed transmitter and receiver filters with impulse responses $h_t^{(l)}(t)$ and $h_r^{(l)}(t)$, respectively, while the lower branch represents the overlay system with transmitter filters with impulse responses $h_t^{(o_1)}(t)$ and $h_t^{(o_2)}(t)$, and receiver filter $h_r^{(o)}(t)$. The signals that are input to the overlay and legacy receivers are corrupted by AWGN sequences $w_1(t)$ and $w_2(t)$, respectively. The legacy system operates over the channel $h_c^{(ll)}(t)$ while the overlay system works over the channel $h_c^{(o_1o)}(t)$ and $h_c^{(o_2o)}(t)$. As shown in the figure, $h_c^{(o_1l)}(t)$, $h_c^{(o_2l)}(t)$, and $h_c^{(lo)}(t)$ represent the crosstalk (interference) between the two systems. The notation for the corresponding quantities is analogous to that used in Table 3.1.

Our objective is to design a wireless system whereby an overlay system can operate simultaneously with a legacy system without waiting for the channel to be vacant by jointly optimizing the overlay transmitters, $h_t^{(o_1)}(t)$ and $h_t^{(o_2)}(t)$, and receiver $h_r^{(o)}(t)$, while simultaneously mitigating interference to the legacy system subject to the constraint

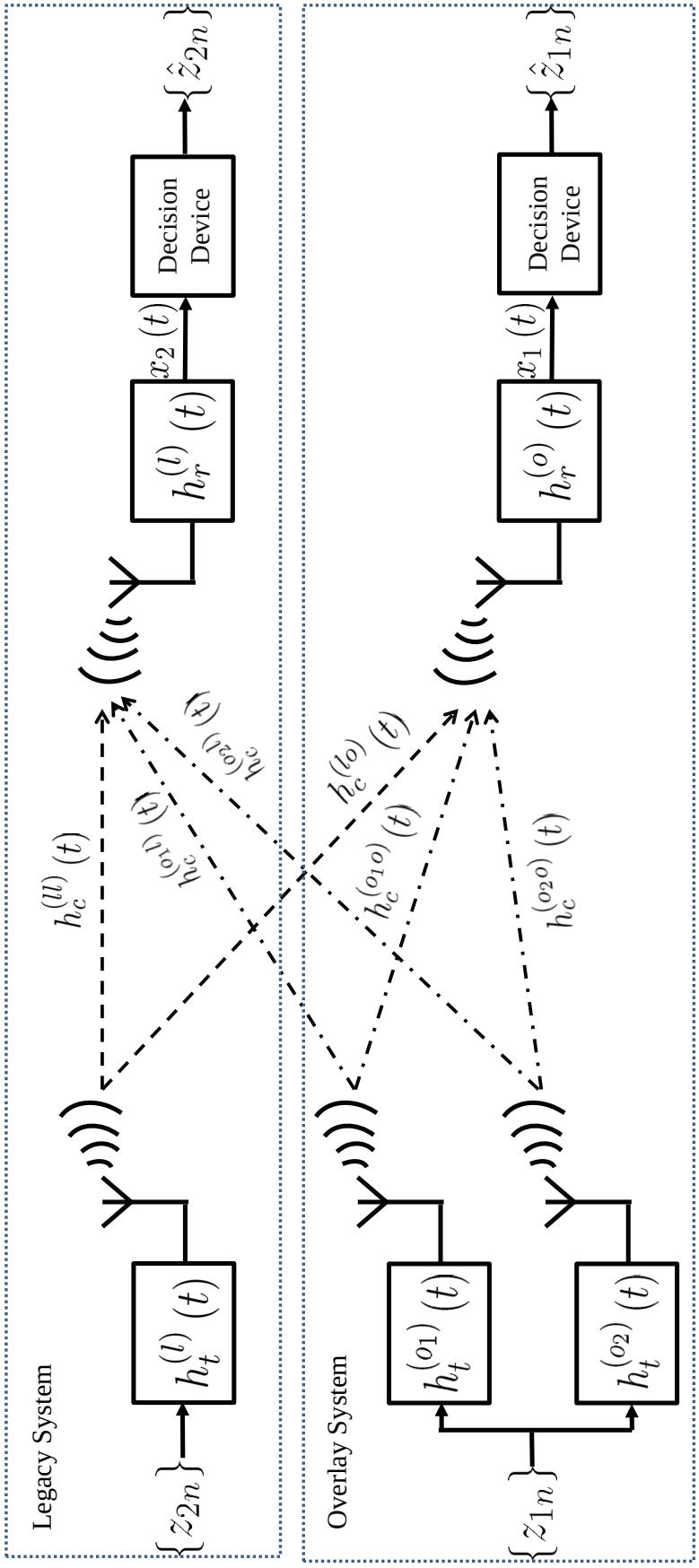

Figure 3.3: Dual-transmit-antenna system model.

that the legacy system has a fixed impulse response. A composite MSE which considers the performance of the new system and the performance degradation of the existing one due to the introduction of the overlay system, is used as a figure of merit. It is assumed that the both systems occupying the same bandwidth.

Given the constraint that the legacy system is fixed and cannot be modified, a composite MSE is given by

$$MSE = MSE_1 + \beta MSE_2^e \tag{3.24}$$

$$\begin{aligned} MSE_1 &\equiv \text{MSE in channel 1 (overlay MSE)} \\ &= E\left[|z_{1n} - \hat{z}_{1n}|^2\right] \end{aligned} \tag{3.25}$$

$$\begin{aligned} MSE_2^e &= \text{legacy excess MSE} \\ &= E\left[|q_{2n}|^2\right] \end{aligned} \tag{3.26}$$

and where

$$q_{2n} \triangleq q_2(t)\Big|_{t=nT} \tag{3.27}$$

$$q_2(t) = \left[h_t^{(o_1)}(t) * h_c^{(o_1 l)}(t) + h_t^{(o_2)}(t) * h_c^{(o_2 l)}(t)\right] * h_r^{(l)}(t) \tag{3.28}$$

The output signals $x_1(t)$ and $x_2(t)$ are produced by processing the signal at the receiver input in the presence of AWGN, $w_1(t)$ and $w_2(t)$, through the receiver filters, $h_r^{(o)}(f)$ and $h_r^{(l)}(f)$, are the input to the decision device to generate the final estimates,

$$\begin{aligned} x_1(t) &= \sum_{n=-\infty}^{\infty} z_{1n} p_{11}(t - nT) \\ &\quad + \sum_{n=-\infty}^{\infty} z_{2n} p_{21}(t - nT) + \upsilon_1(t) \end{aligned} \tag{3.29}$$

$$\upsilon_1(t) = w_1(t) * h_r^{(o)}(t) \tag{3.30}$$

$$S_{\upsilon_1} = N_0 \left| H_r^{(o)}(f) \right|^2 \tag{3.31}$$

where S_{υ_1} denotes the power spectral density of $\upsilon_1(t)$, N_0 is the additive noise power spectral density, and

$$p_{11}(t) = \left[h_t^{(o_1)}(t) * h_c^{(o_1 o)}(t) + h_t^{(o_2)}(t) * h_c^{(o_2 o)}(t) \right] * h_r^{(o)}(t) \tag{3.32}$$

$$p_{21}(t) = h_t^{(l)}(t) * h_c^{(lo)}(t) * h_r^{(o)}(t) \tag{3.33}$$

3.2.2 optimal mmse solution for dual-transmit-antenna overlay system design.

It is assumed that $x_1(t)$ is synchronously sampled at instants nT; the sample at instant $t = 0$ is represented by x_{10} and σ^2 denotes the input symbol variance. Then

$$\begin{aligned} x_{10} &= \sum_{n=-\infty}^{\infty} z_{1n} p_{11}(nT) \\ &\quad + \sum_{n=-\infty}^{\infty} z_{2n} p_{21}(nT) + \upsilon_{10} \end{aligned} \tag{3.34}$$

and the overlay MSE (MSE_1) is given by

$$\begin{aligned} E\left[|x_{10} - Z_{10}|^2 \right] &= \sigma^2 \sum_{n=-\infty}^{\infty} |p_{11}(nT) - \delta_{n0}|^2 \\ &\quad + \sigma^2 \sum_{n} |p_{21}(nT)|^2 \\ &\quad + N_0 \int |\upsilon_{10}|^2 dt \end{aligned} \tag{3.35}$$

which is

$$\begin{aligned} MSE_1 &= E\left[\left|x_{10}-Z_{10}\right|^2\right] \\ &= \frac{\sigma^2}{T}\int_{-\frac{1}{2T}}^{\frac{1}{2T}}\left|\left[H_t^{(o_1)}(f)\,H_c^{(o_1o)}(f)+H_t^{(o_2)}(f)\,H_c^{(o_2o)}(f)\right]H_r^{(o)}(f)-T\right|^2 \\ &\quad+\frac{\sigma^2}{T}\int_{-\frac{1}{2T}}^{\frac{1}{2T}}\left|H_t^{(l)}(f)\,H_c^{(lo)}(f)\,H_r^{(o)}(f)\right|^2 df \\ &\quad+N_0\int_{-\frac{1}{2T}}^{\frac{1}{2T}}\left|H_r^{(o)}(f)\right|^2 df \end{aligned} \tag{3.36}$$

The legacy excess MSE can be written as

$$MSE_2^e=\frac{\sigma^2}{T}\int_{-\frac{1}{2T}}^{\frac{1}{2T}}\left|\left[H_t^{(o_1)}(f)\,H_c^{(o_1l)}(f)+H_t^{(o_2)}(f)\,H_c^{(o_2l)}(f)\right]H_r^{(l)}(f)\right|^2 df \tag{3.37}$$

The average transmitter power on the overlay user is

$$P_t=P_{t1}+P_{t2} \tag{3.38}$$

where P_{t1} and P_{t2} represent the average transmitter power from the first and the second antenna of the overlay system, respectively, and

$$P_{t1}=\frac{\sigma^2}{T}\int_{-\frac{1}{2T}}^{\frac{1}{2T}}\left|H_t^{(o_1)}(f)\right|^2 df \tag{3.39}$$

$$P_{t2}=\frac{\sigma^2}{T}\int_{-\frac{1}{2T}}^{\frac{1}{2T}}\left|H_t^{(o_2)}(f)\right|^2 df \tag{3.40}$$

The optimization problem of optimizing (3.24) subject to the average power constraint in (3.38) can be rewritten as below by introducing Lagrange multipliers λ_1 and λ_2

$$MSE=MSE_1+\beta MSE_2^e+\lambda_1 P_{t1}+\lambda_2 P_{t2} \tag{3.41}$$

Substituting (3.36)–(3.40) into (3.41)

$$\begin{aligned} MSE &= \frac{\sigma^2}{T}\int_{-\frac{1}{2T}}^{\frac{1}{2T}} \left|\left[H_t^{(o_1)}(f)\,H_c^{(o_1o)}(f)+H_t^{(o_2)}(f)\,H_c^{(o_2o)}(f)\right]H_r^{(o)}(f)-T\right|^2 \\ &+\frac{\sigma^2}{T}\int_{-\frac{1}{2T}}^{\frac{1}{2T}}\left|H_t^{(l)}(f)\,H_c^{(lo)}(f)\,H_r^{(o)}(f)\right|^2 df \\ &+N_0\int_{-\frac{1}{2T}}^{\frac{1}{2T}}\left|H_r^{(o)}(f)\right|^2 df \\ &+\beta\frac{\sigma^2}{T}\int_{-\frac{1}{2T}}^{\frac{1}{2T}}\left|\left[H_t^{(o_1)}(f)\,H_c^{(o_1l)}(f)+H_t^{(o_2)}(f)\,H_c^{(o_2l)}(f)\right]H_r^{(l)}(f)\right|^2 df \\ &+\frac{\sigma^2}{T}\int_{-\frac{1}{2T}}^{\frac{1}{2T}}\left[\lambda_1\left|H_t^{(o_1)}(f)\right|^2+\lambda_2\left|H_t^{(o_2)}(f)\right|^2\right]df \end{aligned} \tag{3.42}$$

Defining the following parameters

$$\mathbf{H_t^{(o)}}=\begin{bmatrix} H_t^{(o_1)}(f)\\ H_t^{(o_2)}(f)\end{bmatrix},\ \mathbf{H_c^{(oo)}}=\begin{bmatrix} H_c^{(o_1o)}(f)\\ H_c^{(o_2o)}(f)\end{bmatrix},\ \mathbf{H_c^{(ol)}}=\begin{bmatrix} H_c^{(o_1l)}(f)\\ H_c^{(o_2l)}(f)\end{bmatrix} \tag{3.43}$$

and

$$\boldsymbol{\lambda}=\mathrm{diag}\left[\lambda_1,\lambda_2\right] \tag{3.44}$$

In what follows, for simplicity of presentation the explicit frequency dependence of the capitalized terms is suppressed. Substituting (3.43) and (3.44) into (3.42)

$$\begin{aligned} MSE &= \frac{\sigma^2}{T}\int_{-\frac{1}{2T}}^{\frac{1}{2T}}\left|\mathbf{H_t^{(o)\intercal}}\mathbf{H_c^{(oo)}}H_r^{(o)}-T\right|^2 df \\ &+\frac{\sigma^2}{T}\int_{-\frac{1}{2T}}^{\frac{1}{2T}}\left|H_t^{(l)}H_c^{(lo)}H_r^{(o)}\right|^2 df \\ &+N_0\int_{-\frac{1}{2T}}^{\frac{1}{2T}}\left|H_r^{(o)}\right|^2 df \\ &+\beta\frac{\sigma^2}{T}\int_{-\frac{1}{2T}}^{\frac{1}{2T}}\left|\mathbf{H_t^{(o)\intercal}}\mathbf{H_c^{(ol)}}H_r^{(l)}\right|^2 df \\ &+\frac{\sigma^2}{T}\int_{-\frac{1}{2T}}^{\frac{1}{2T}}\left[\mathbf{H_t^{(o)\intercal}}\boldsymbol{\lambda}^{\intercal}\mathbf{H_t^{(o)}}\right]df \end{aligned} \tag{3.45}$$

where $^{\intercal}$ denotes the Hermitian transpose operation.

Our goal is to find the optimum $\mathbf{H_t^{(o)}}$ and $H_r^{(o)}$ which result in the minimum MSE. After extensive manipulation, which is provided in Appendix A.1, the following optimality conditions are obtained

$$\mathbf{H_t^{(o)\intercal}} \mathbf{M_1} \mathbf{H_t^{(o)}} = \left| H_r^{(o)} \right|^2 M_2 \tag{3.46}$$

$$\left[\mathbf{H_t^{(o)\intercal}} \mathbf{M_3} \mathbf{H_t^{(o)}} + M_2 \right] H_r^{(o)} = T \mathbf{H_t^{(o)\intercal}} \mathbf{H_c^{(oo)}} \tag{3.47}$$

Algorithm 2 Dual-transmit-antenna program pseudo code

```
Choose an initial value for λ1 and λ2.
Select total desired transmitter power level P.
Select desired transmitter power level from the first overlay transmitting antenna (P1),
    and from the second one (P2) such that P = P1 + P2
Select tolerance power level δ (typically δ = 0.1 dB)
for fn ∈ [−1/2T,1/2T] do
    while |Pt1 − P1| > δ or |Pt2 − P2| > δ do
        Compute optimal transmitter/receiver from (3.46) and (3.48) numerically.
        Compute the first antenna transmitter power (Pt1) from (3.39).
        Compute the second antenna transmitter power (Pt2) from (3.40).
        if Pt1 > P1 then
            Increase λ1.
        else
            Decrease λ1.
        end if
        if Pt2 > P2 then
            Increase λ2.
        else
            Decrease λ2.
        end if
    end while
    Compute the optimum MSE from (3.41).
end for
```

$$\left[\left| H_r^{(o)} \right|^2 \mathbf{M_3} + \mathbf{M_1} \right] \mathbf{H_t^{(o)}} = T H_r^{(o)} \mathbf{H_c^{(oo)}} \tag{3.48}$$

where

$$\mathbf{M_1} = \beta \left| H_r^{(l)} \right|^2 \mathbf{H_c^{(ol)}} \mathbf{H_c^{(ol)^\intercal}} + \boldsymbol{\lambda} \tag{3.49}$$

$$M_2 = \left| H_t^{(l)} \right|^2 \left| H_c^{(lo)} \right|^2 + \eta^{-1} \tag{3.50}$$

$$\mathbf{M_3} = \mathbf{H_c^{(oo)}} \mathbf{H_c^{(oo)^\intercal}} \tag{3.51}$$

Equations (3.46), (3.47), and (3.48) do not have a closed-form solution for $\mathbf{H_t^{(o)}}$ and $H_r^{(o)}$. Therefore, a numerical optimization algorithm is used to find the optimum overlay receiver ($H_r^{(o)}$). The resultant receiver response is then applied to (3.48) in order to find the optimum overlay transmitter ($\mathbf{H_t^{(o)}}$) as indicated in the pseudo code in Algorithm 2.

Line 6–20 in Algorithm 2 is an efficient iterative way to find the approximate values for the Lagrange multipliers λ_1 and λ_2 that satisfy the desired power constraint. However, because the optimization is not done in a joint manner, the resulting solution is not necessarily optimum; thus, we can seek a numerical joint optimization of λ_1 and λ_2. While this is computationally more intense, it should yield to better performance as verified in Section 4.2.

Chapter 4

Analytical and Simulation Results

In this chapter, we present simulation results that show the efficiency of our solution in designing the overlay system over a flat Rayleigh fading channel in the presence of AWGN for the following cases :

Case 1: Both the overlay and the legacy systems are under *strong* interference.

Case 2: The *overlay* system experiences *weaker* interference than the legacy system ($h_c^{(ol)}(t) > h_c^{(lo)}(t)$).

Case 3: The *overlay* system experiences *stronger* interference than the legacy system ($h_c^{(ol)}(t) < h_c^{(lo)}(t)$).

Case 4: Both the overlay and the legacy systems are under *weak* interference.

In all cases without loss of generality we assume both the legacy and the overlay system occupy a bandwidth of 15 MHz and the legacy transmitter power is 0 dB.

4.1 Single-Transmit-Antenna System

Figure 4.1 shows an example of the overall transfer function (including the transmitter, channel, and the receiver) of the legacy system and that of the overlay system optimized for a given channel conditions. It is clear that the overall transfer function of the legacy system is flat which indicates that the legacy system performance is optimized. On the other hand,

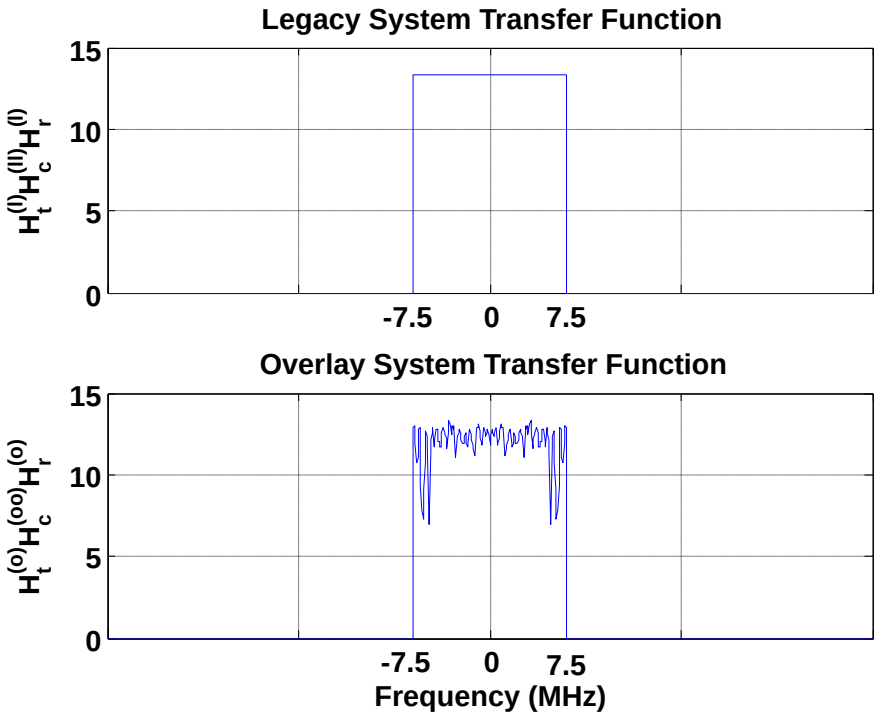

Figure 4.1: Example of overlay and legacy overall transfer functions.

the overall transfer function of the overlay system is not flat due to optimization of the overlay system to minimize the interference to the existing legacy system.

4.1.1 mse performance.

In this section, we compare the effects of varying key parameters such as the overlay transmitter power and the amount of overlap between the legacy and the overlay systems on the designed optimized system with the un-optimized one (when the transmitter and receiver of the overlay system are simply matched filters).

The performance of the designed optimized overlay system as a function of its transmitted power, when both legacy and overlay systems are completely overlapped in the first Nyquist zone, and $\beta = 1$, for a fixed legacy system compared to an un-optimized one is investigated in Figure 4.2–4.5. As we see in the figures, for different channel scenarios increasing the overlay power reduces the overlay MSE but degrades the legacy performance for both the optimized and un-optimized systems due to the increased crosstalk

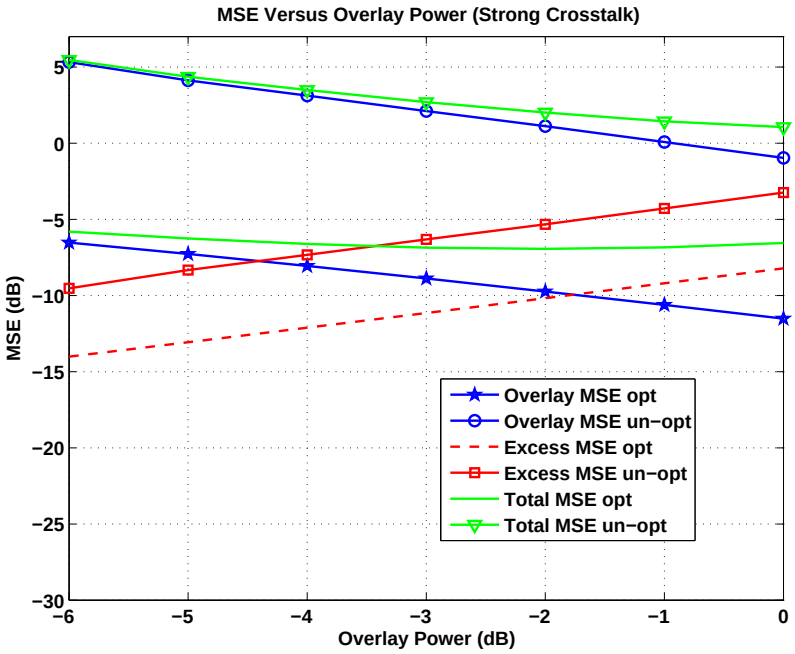

Figure 4.2: Effect of varying overlay power in an optimized system and un-optimized one for Case 1.

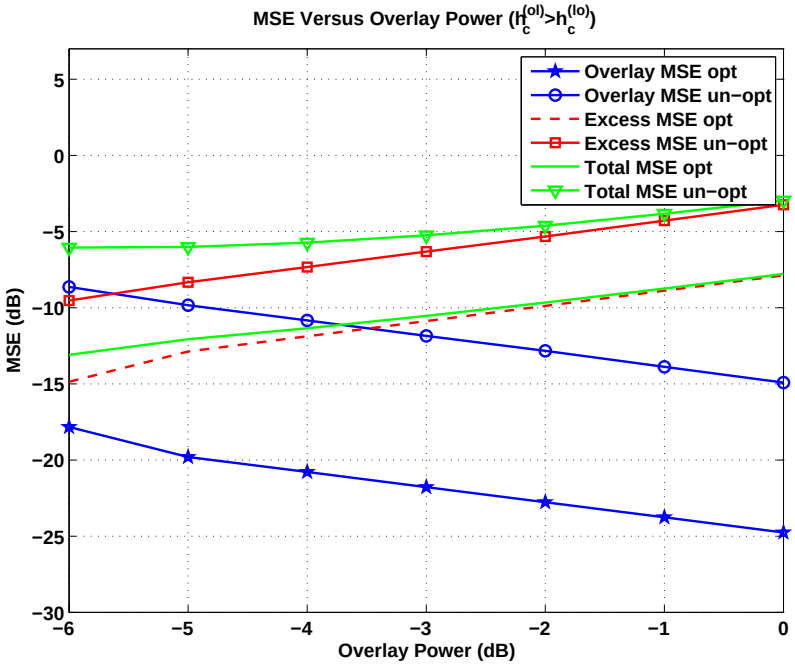

Figure 4.3: Effect of varying overlay power in an optimized system and un-optimized one for Case 2.

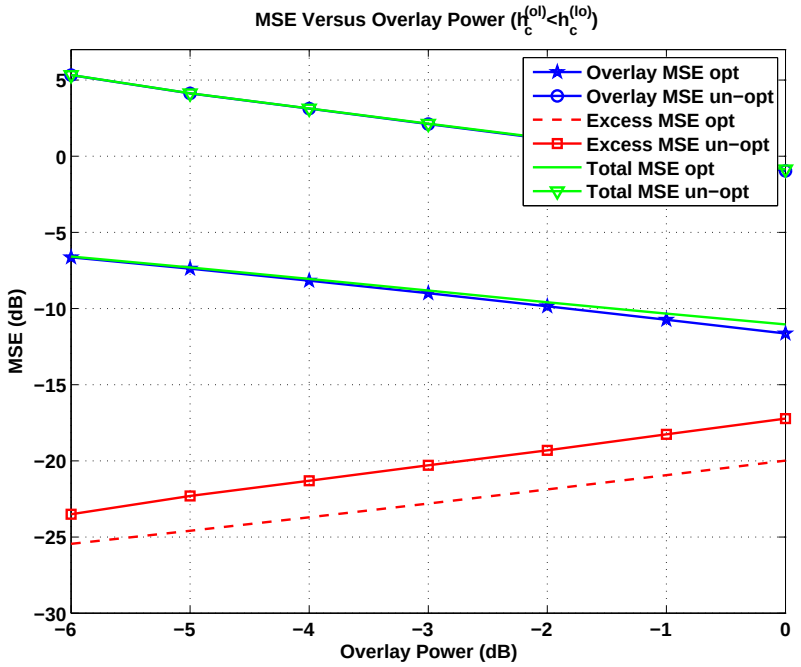

Figure 4.4: Effect of varying overlay power in an optimized system and un-optimized one for Case 3.

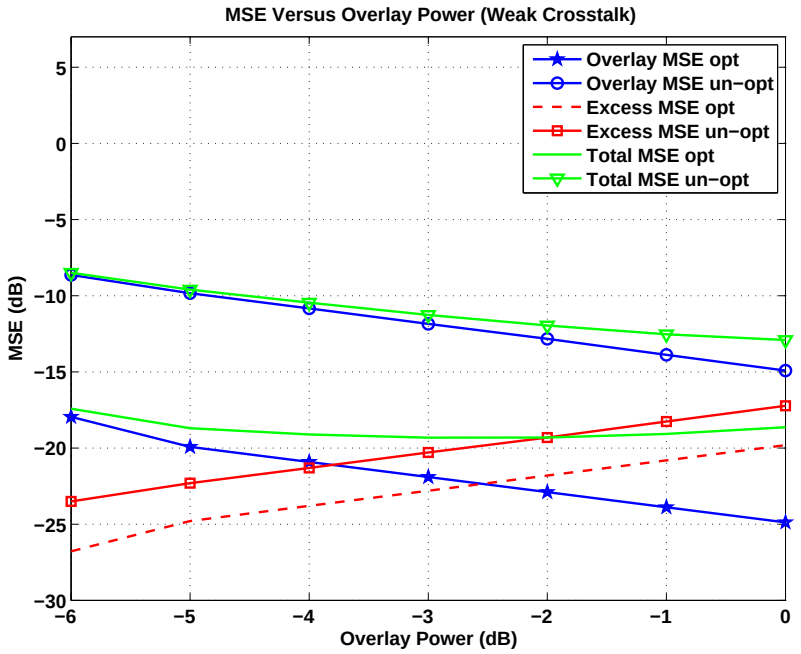

Figure 4.5: Effect of varying overlay power in an optimized system and un-optimized one for Case 4.

levels caused by more overlay transmitter power. Furthermore, as we observe in Figure 4.3 the system is dominated by the interference to the legacy system (Case 2) that is why relative to Figure 4.4, we have higher legacy MSE and lower overlay MSE. The results also show that the optimization provides a significant performance gain by reducing the MSE by about 10 dB that indicates the optimization of the self-performance and mitigation of interference to the legacy system.

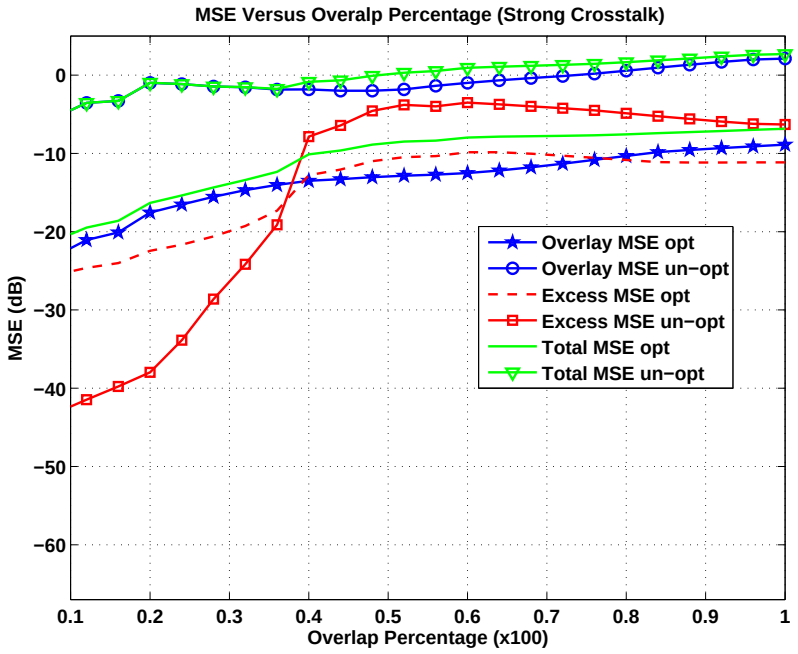

Figure 4.6: Effect of varying percentage overlap between the legacy and the overlay systems in an optimized and un-optimized systems for Case 1.

Figure 4.6–4.9 show the variations of the excess, overlay and total MSE as a function of the amount of overlap between the legacy and the overlay systems. Cases for the optimized and un-optimized systems are shown for an overlay power of -3 dB and $\beta = 1$. As seen in the figure, for different scenarios by increasing the degree of overlap between the legacy and the overlay systems there is an increase in the interference which leads to the degradation of the system performance. Moreover, in Figure 4.7 (Case 2) higher legacy MSE and lower overlay MSE are observed compared to Figure 4.8 (Case 3) since the system is dominated by the interference to the legacy system.

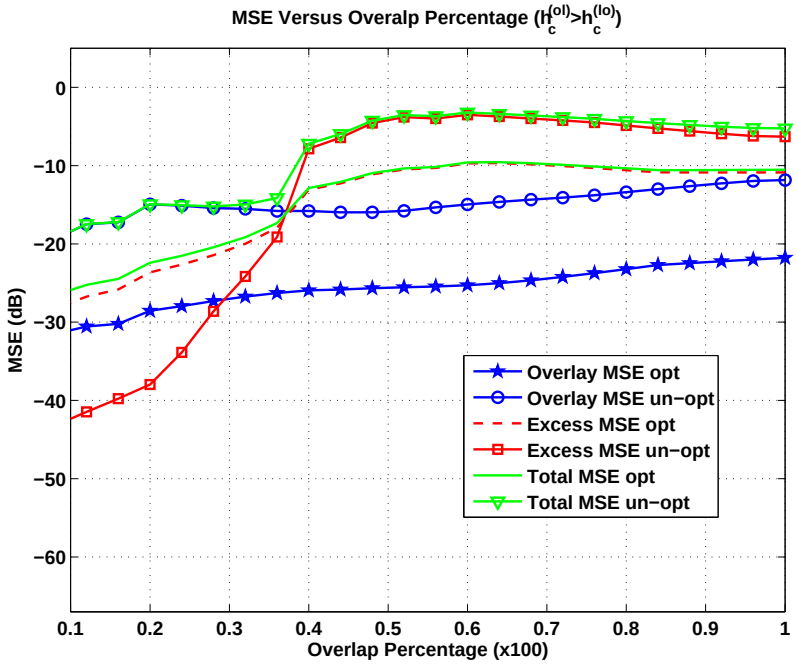

Figure 4.7: Effect of varying percentage overlap between the legacy and the overlay systems in an optimized and un-optimized systems for Case 2.

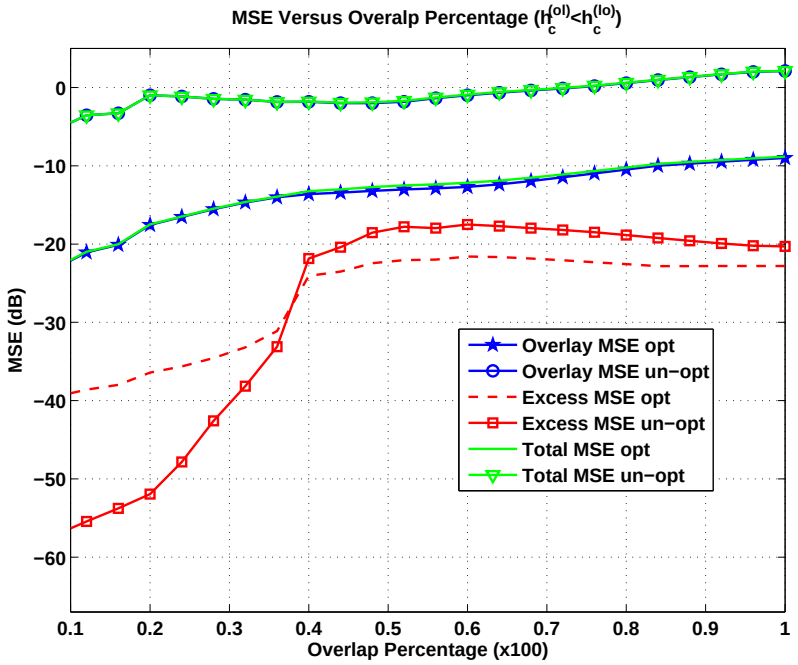

Figure 4.8: Effect of varying percentage overlap between the legacy and the overlay systems in an optimized and un-optimized systems for Case 3.

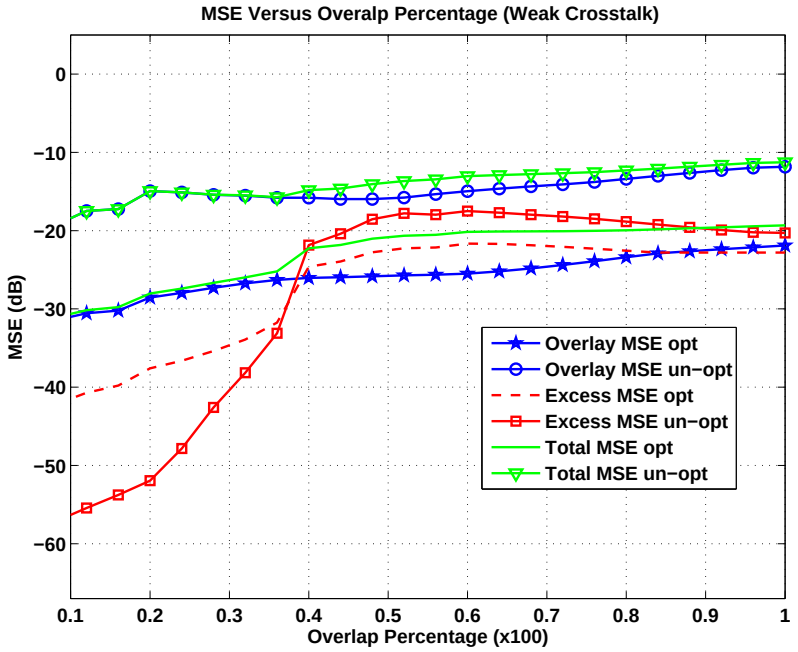

Figure 4.9: Effect of varying percentage overlap between the legacy and the overlay systems in an optimized and un-optimized systems for Case 4.

In Figure 4.10–4.13 we show the variations of total MSE and the overlay MSE with the overlay power and the amount of overlap between the legacy and the overlay systems, when both are under strong interference and both are under weak interference, for the optimized and the un-optimized systems when $\beta = 1$. In all cases, we observe for different power levels and for higher amount of overlap between the two systems, the optimized system perform about 10 dB better than un-optimized one which implies a significant gain performance of our designed system.

Figure 4.14–4.15 depict the variations of excess MSE as a function of the overlay power and the degree of overlap between the legacy and the overlay systems for both the optimized and the un-optimized systems under strong and weak crosstalk levels . The results show that the optimized system performs better than the un-optimized one by increasing the amount of overlap between the overlay and the legacy systems.

The performance of the designed overlay system as a function of the relative weight in the optimization problem (β), when both legacy and overlay systems are completely

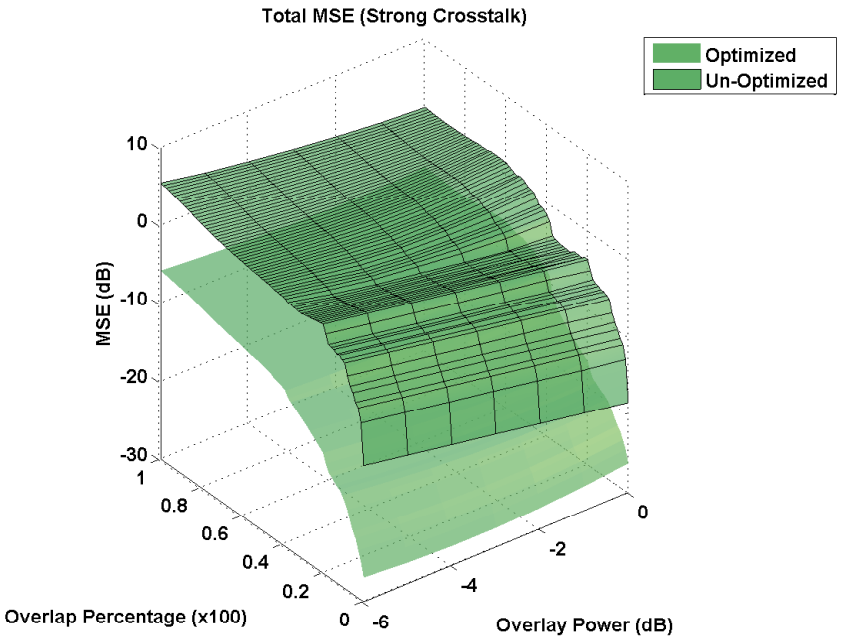

Figure 4.10: Effect of varying percentage overlap and the overlay power on total MSE in an optimized and un-optimized systems for Case 1.

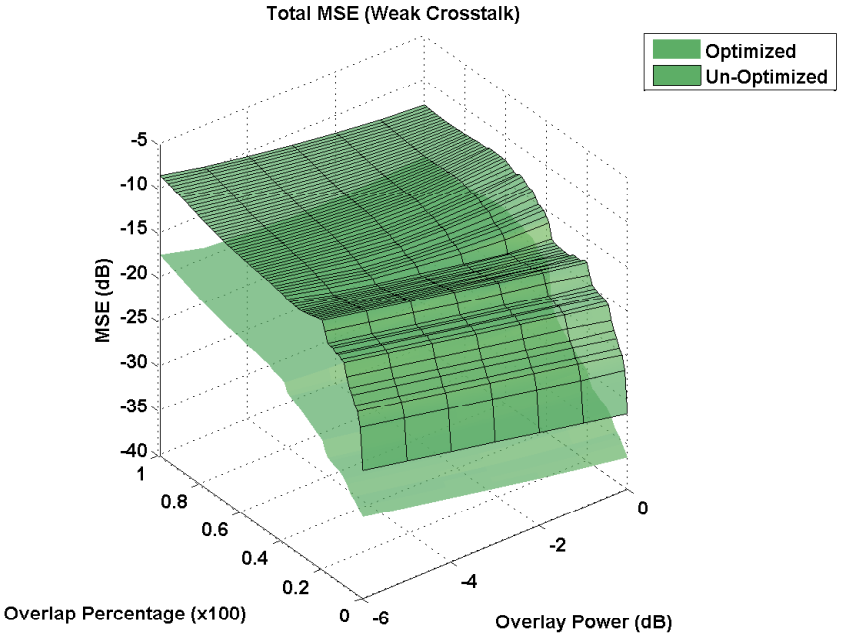

Figure 4.11: Effect of varying percentage overlap and the overlay power on total MSE in an optimized and un-optimized systems for Case 4.

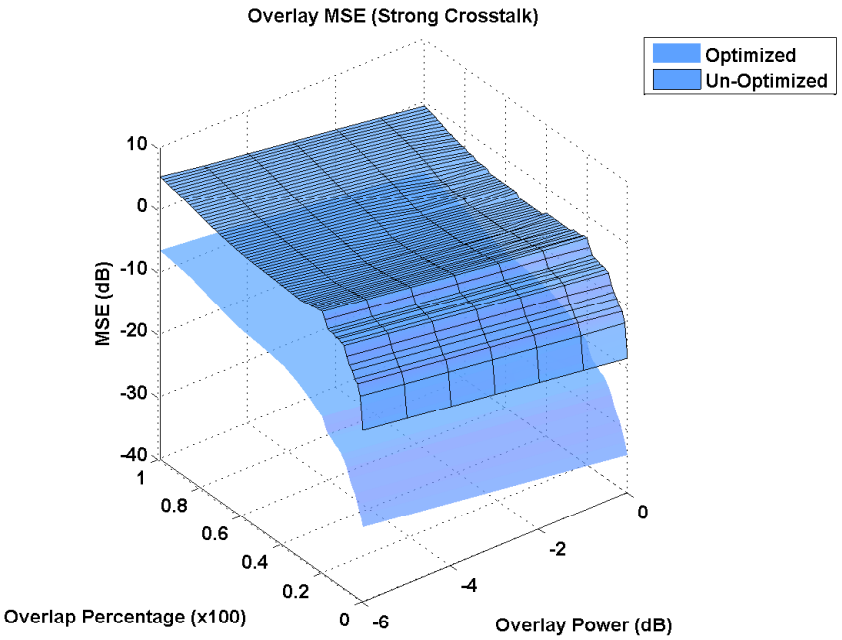

Figure 4.12: Effect of varying percentage overlap and the overlay power on overlay MSE in an optimized and un-optimized systems for Case 1.

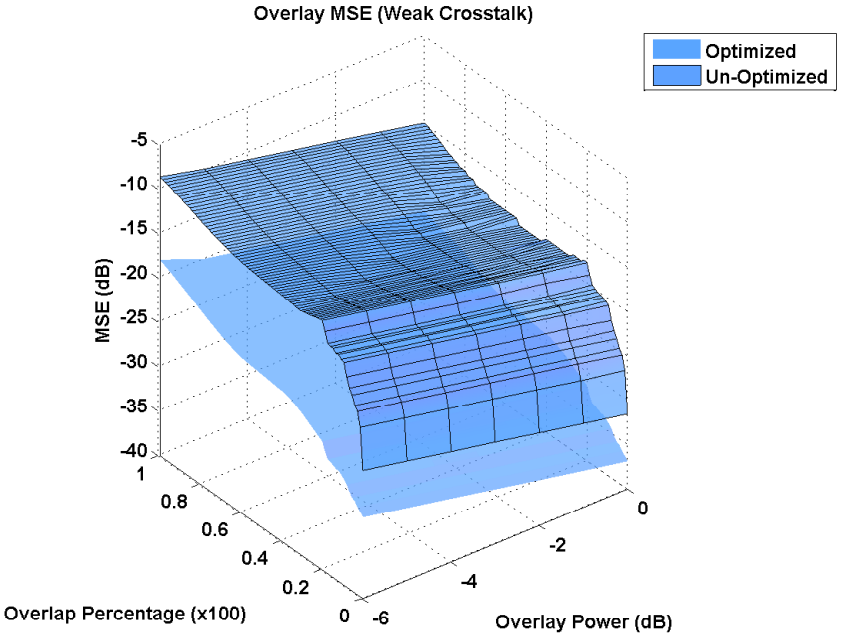

Figure 4.13: Effect of varying percentage overlap and the overlay power on overlay MSE in an optimized and un-optimized systems for Case 4.

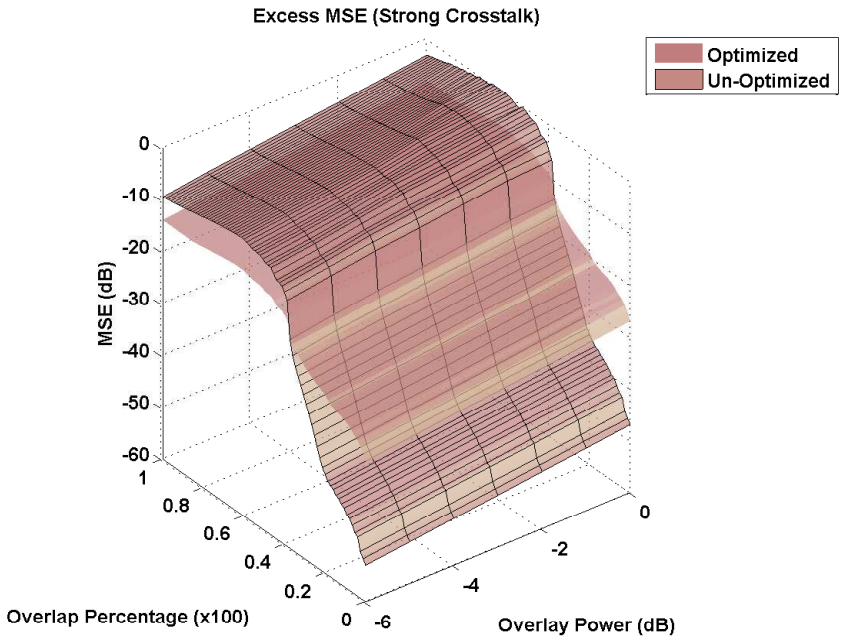

Figure 4.14: Effect of varying percentage overlap and the overlay power on legacy excess MSE in an optimized and un-optimized systems for Case 1.

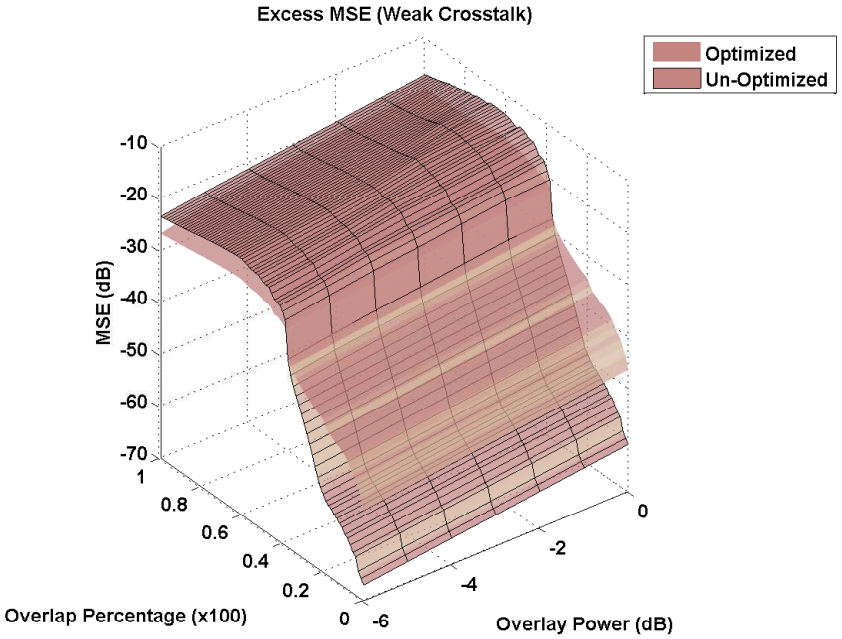

Figure 4.15: Effect of varying percentage overlap and the overlay power on legacy excess MSE in an optimized and un-optimized systems for Case 4.

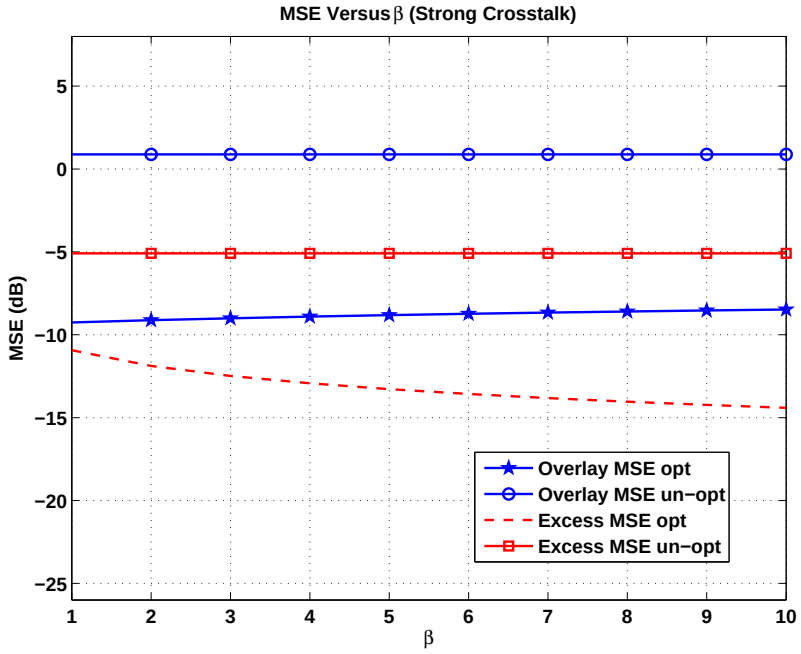

Figure 4.16: Effect of varying the relative weight in the optimization problem (β) in an optimized system and un-optimized one for Case 1.

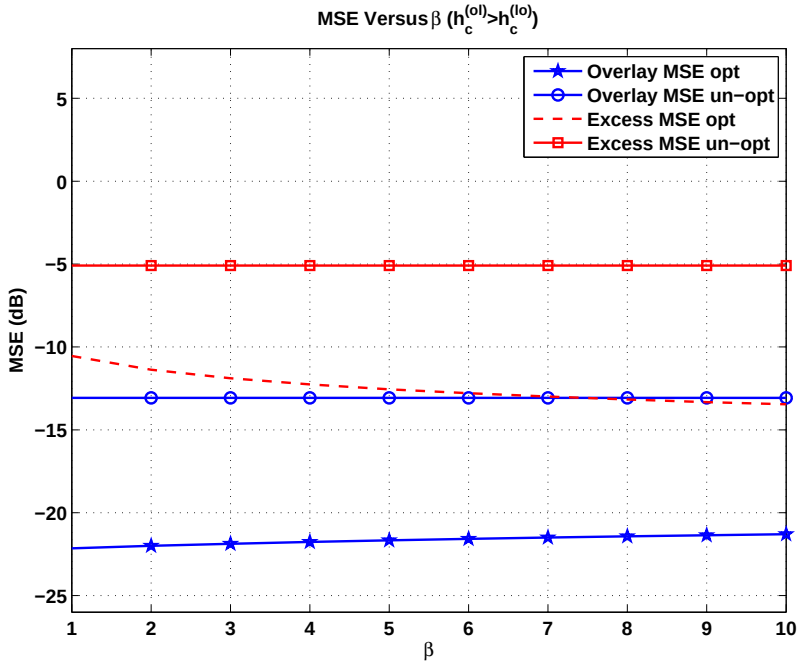

Figure 4.17: Effect of varying the relative weight in the optimization problem (β) in an optimized system and un-optimized one for Case 2.

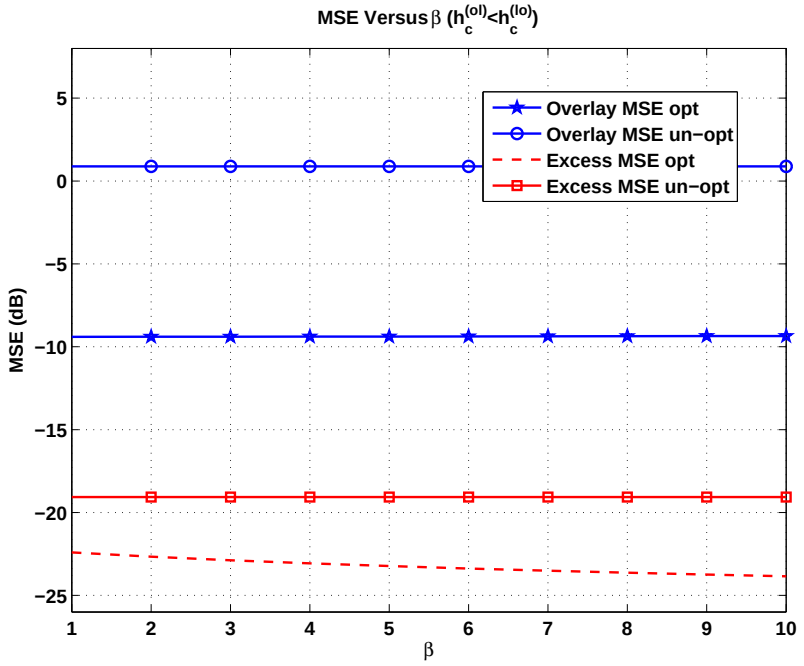

Figure 4.18: Effect of varying the relative weight in the optimization problem (β) in an optimized system and un-optimized one for Case 3.

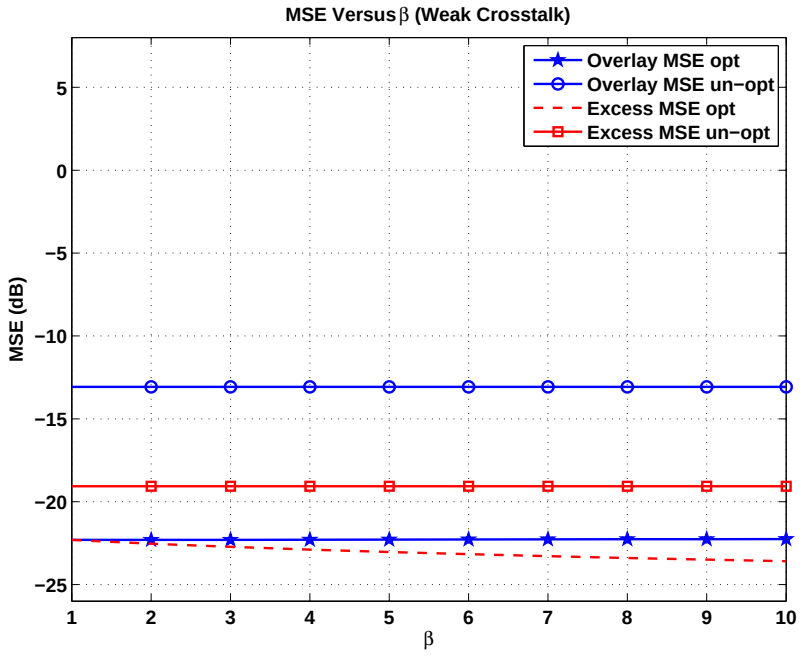

Figure 4.19: Effect of varying the relative weight in the optimization problem (β) in an optimized system and un-optimized one for Case 4.

overlapped in the first Nyquist zone, and the overlay power is fixed at -3 dB, for different channel conditions is shown in Figure 4.16–4.19. We observe that the overlay MSE is relatively insensitive to the variation in β while the excess MSE improves by increasing β, since its impact is stressed more in the optimization problem. Further, when the legacy system is under more interference (Figure 4.16–4.17), the legacy excess MSE is more sensitive to the variations of β, and for higher value of β a gain of 10 dB is achieved, while when it is under weak interference (Figure 4.18–4.19), a maximum gain of 5 dB is attained.

4.1.2 sensitivity to snr estimation.

In this section we investigate the sensitivity of the designed overlay system to the estimation of signal to noise ratio. We first optimize the system for a particular SNR and then compute the incurred loss in MSE by using the system in the presence of different SNR levels. Throughout the simulations, we assume that the overlay transmitter power is fixed at -3 dB, the signal energy is normalized to unity, and the noise energy is varied.

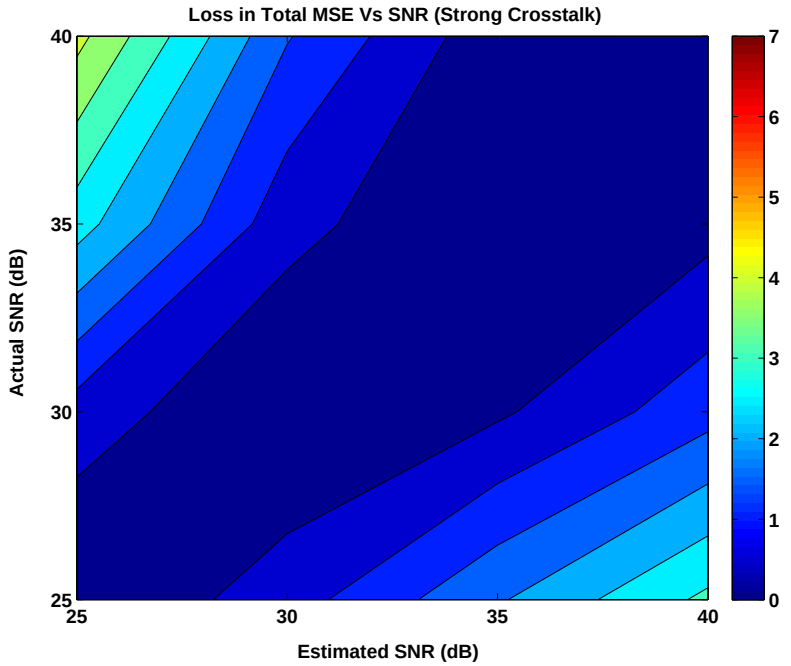

Figure 4.20: Loss in the total MSE with SNR estimation for Case 1.

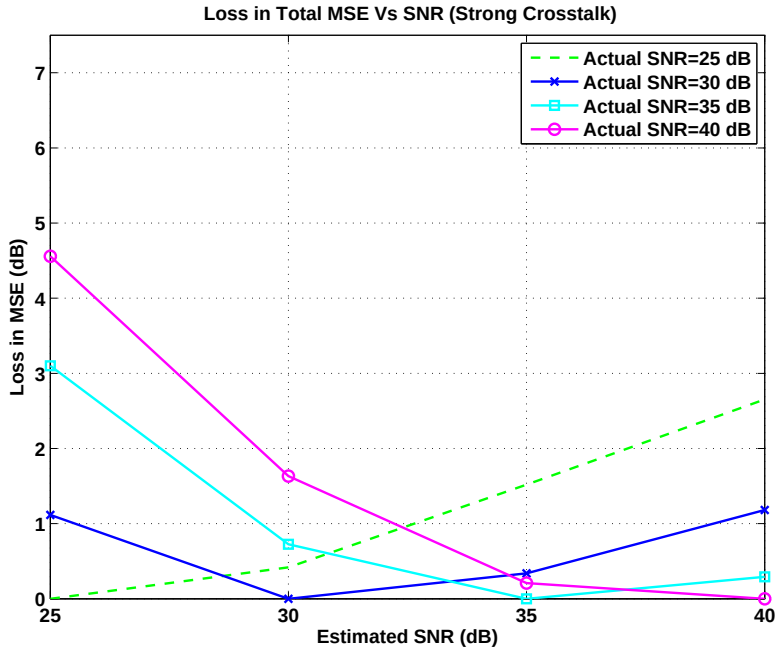

Figure 4.21: Loss in the total MSE at particular actual SNR values for Case 1.

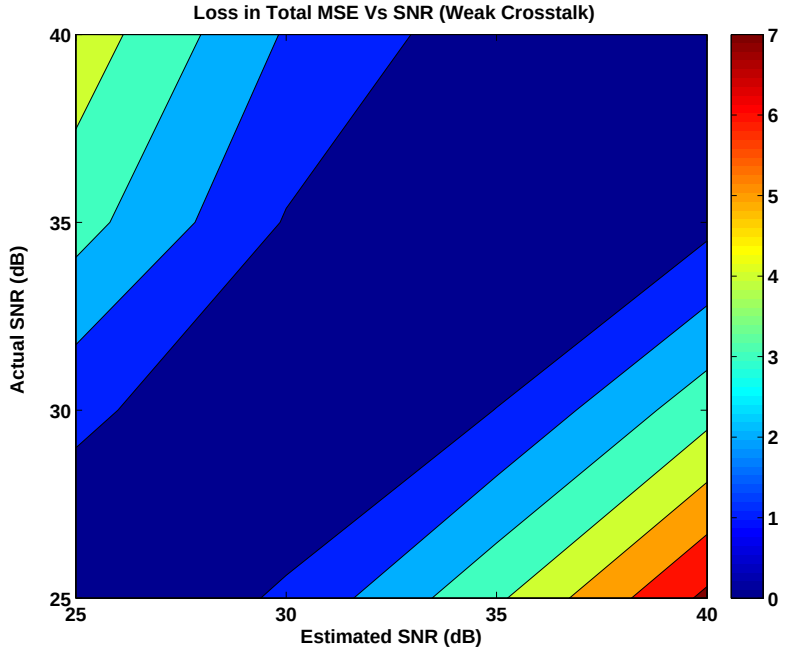

Figure 4.22: Loss in the total MSE with SNR estimation for Case 4.

Figure 4.20–4.23 demonstrate the incurred loss in total MSE of the system as a function of its SNR for strong and weak crosstalk scenarios. We see that the system has

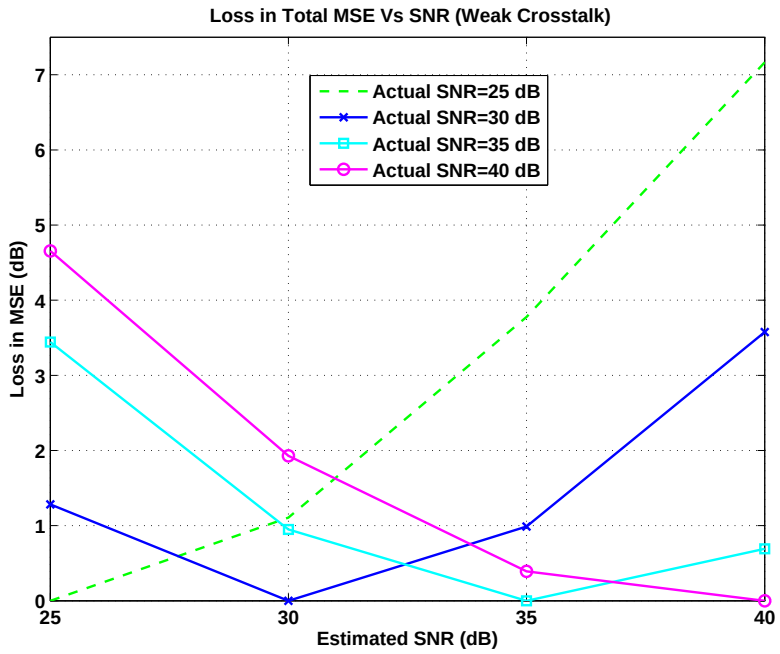

Figure 4.23: Loss in the total MSE at particular actual SNR values for Case 4.

its no loss (0 dB) when it is used for its optimized condition. For the strong interference case, a maximum loss of 4.5 dB is incurred, while in the weak crosstalk case, the maximum incurred loss is 7 dB. The results show that even if the SNR estimation is not accurate, the system can still provide good performance compared to un-optimized system even for a significant error in the actual SNR compared to the estimated SNR.

4.1.3 sensitivity to channel estimation.

Figure 4.24–4.27 compares the overlay MSE, the excess MSE, and the total MSE of our designed optimum system using actual channels (perfect channel knowledge) with the optimum system using the estimated channels for different channel estimate MSEs. The overlay transmitter power is fixed at -3 dB, and $\beta = 1$. As we observe, the system performance degrades as the channel estimates become more inaccurate. In addition, under different channel conditions the estimated excess MSE is fairly insensitive to the error in the channel estimation, and with a maximum channel estimate error of -15 dB, the estimated overlay MSE degrades by approximately 4 dB only. The results indicate minimal

degradation in the performance of the system even under poor channel estimation.

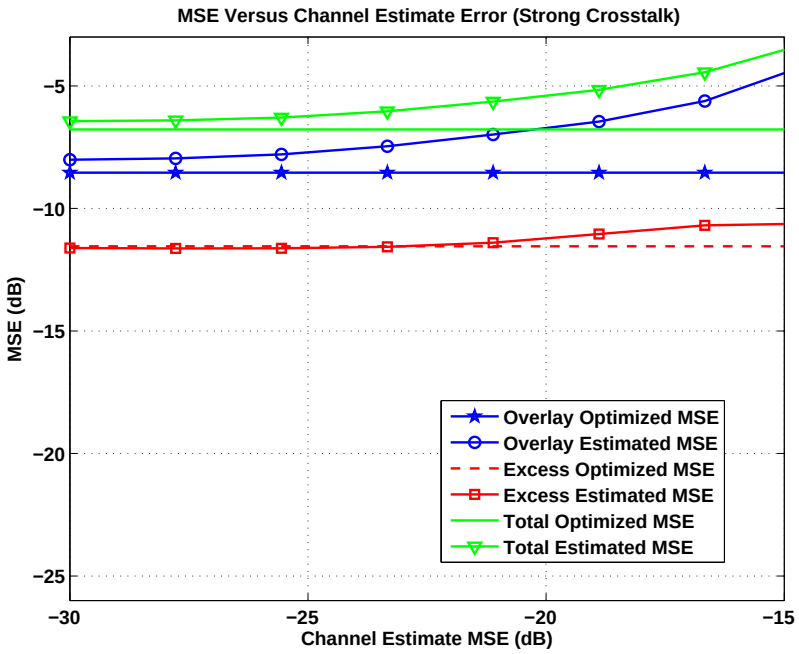

Figure 4.24: Comparison between the performance of an optimized system using actual channels, with optimized system using estimated channels for Case 1.

In Figure 4.28–4.31 we compare the performance of the optimized system as a function of the overlay power using actual channels with the optimum system using the estimated channels when the channel estimate MSE is -20 dB. As seen in Figure 4.28–4.31, for different channel scenarios and under different overlay transmitter power levels the overall system performance degrades by maximum 2 dB only.

4.1.4 non-joint optimization.

So far, we have explored the joint transmitter/receiver optimization for the overlay system, however, from the practical standpoint it is maybe more practical to fix either the overlay transmitter or its receiver and optimize its receiver or transmitter, respectively. In this section we study the performance loss which will be incurred due to not performing the joint optimization.

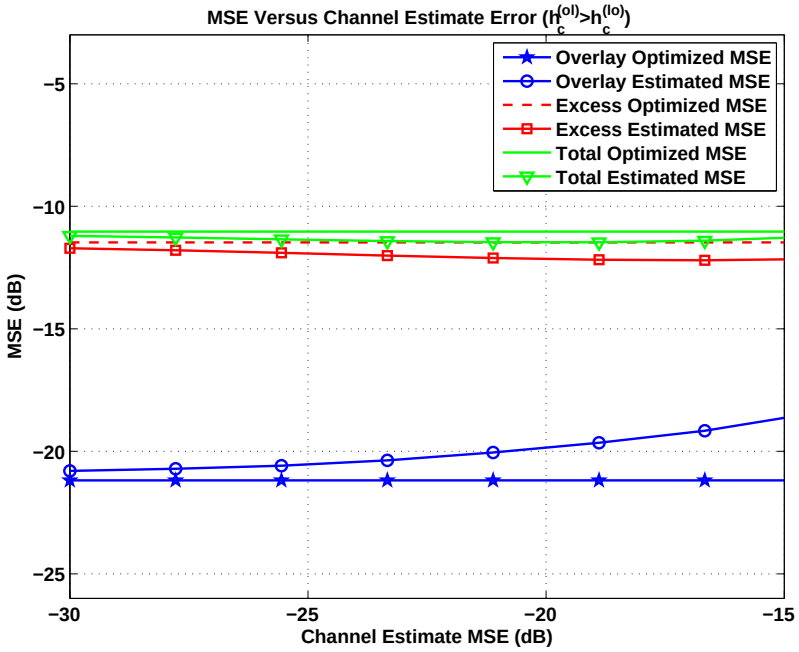

Figure 4.25: Comparison between the performance of an optimized system using actual channels, with optimized system using estimated channels for Case 2.

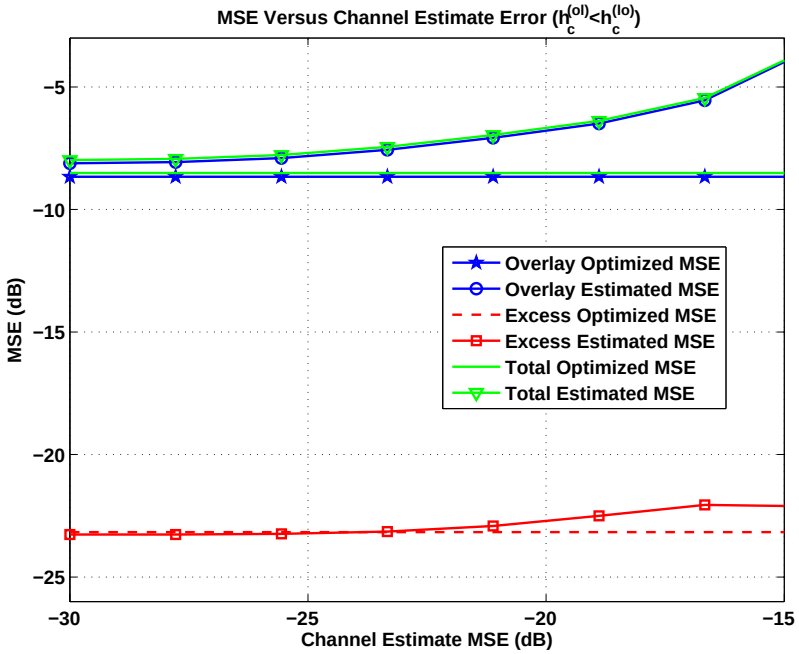

Figure 4.26: Comparison between the performance of an optimized system using actual channels, with optimized system using estimated channels for Case 3.

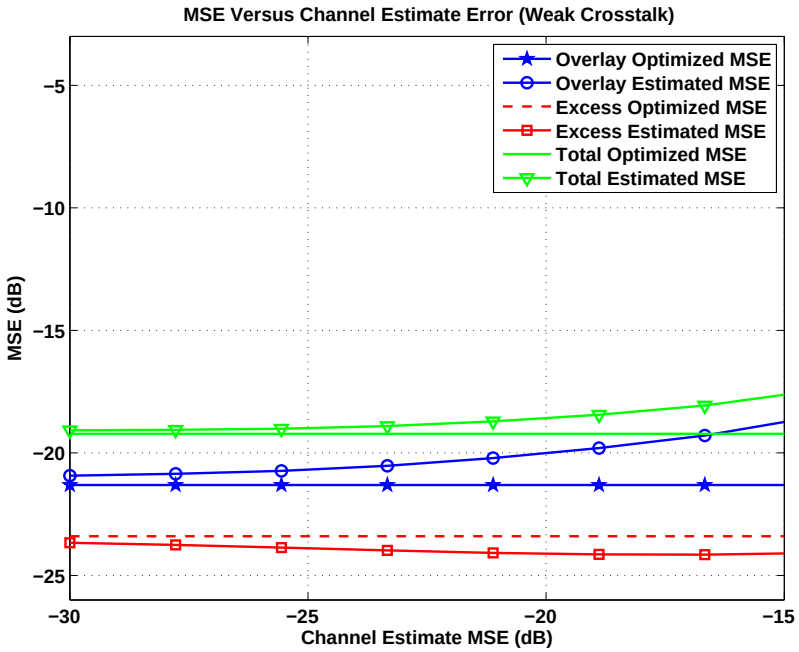

Figure 4.27: Comparison between the performance of an optimized system using actual channels, with optimized system using estimated channels for Case 4.

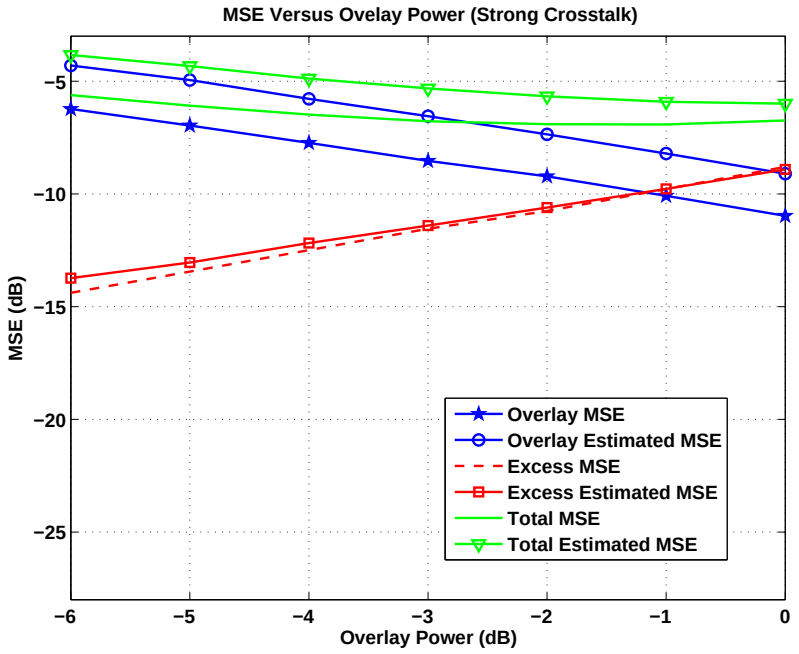

Figure 4.28: MSE as a function of overlay transmitter power for an optimized system using actual channels, and optimized system using estimated channels for Case 1.

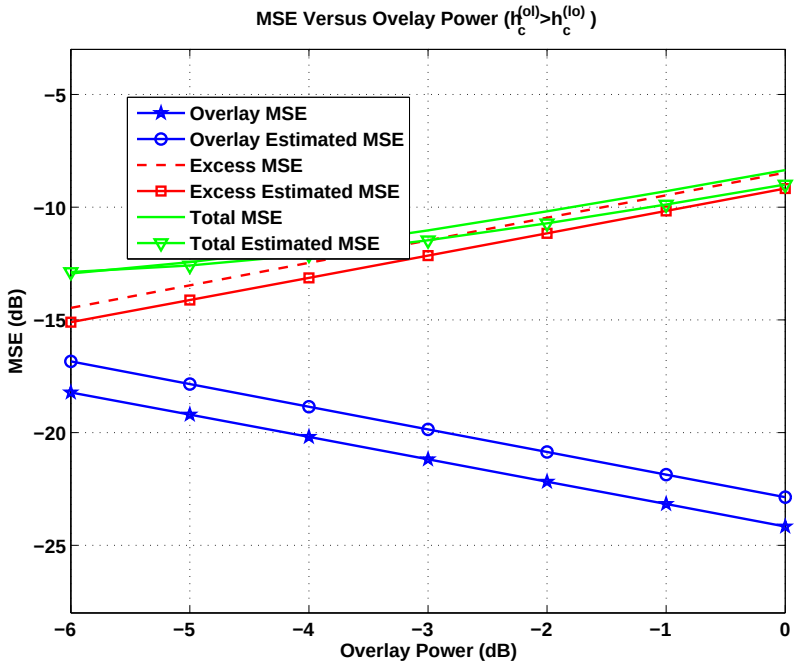

Figure 4.29: MSE as a function of overlay transmitter power for an optimized system using actual channels, and optimized system using estimated channels for Case 2.

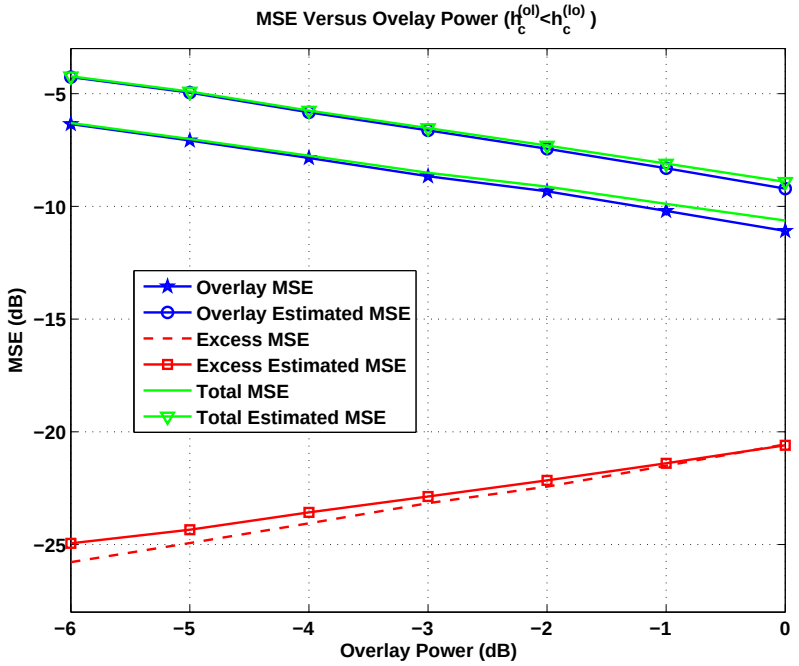

Figure 4.30: MSE as a function of overlay transmitter power for an optimized system using actual channels, and optimized system using estimated channels for Case 3.

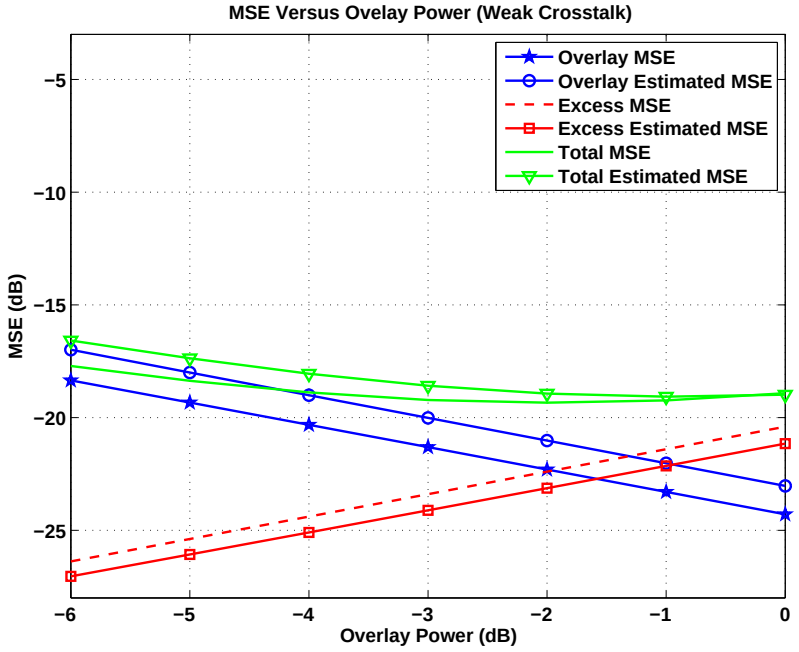

Figure 4.31: MSE as a function of overlay transmitter power for an optimized system using actual channels, and optimized system using estimated channels for Case 4.

Figure 4.32-4.33 compare the performance of a system when its overlay transmitter/receiver are jointly optimized, with a system having a transmitter-optimized overlay, and a an un-optimized system, when the overlay system is under strong interference. We observe that the legacy excess MSE is fairly insensitive to the transmitter-only optimization. However, optimizing the overlay transmitter only leads to a significant degradation of the overlay system performance.

The performance of a system with a jointly optimized transmitter/receiver overlay, a system with a receiver-optimized overlay, and a an un-optimized system, when the overlay system is under strong interference, are compared in Figure 4.34-4.35. The results show that for receiver-only optimization is a sub-optimum solution and for a -3 dB overlay transmitter power, a total MSE loss of about -5 dB, compared to the joint optimized case, is incurred. Moreover, comparing Figure 4.32-4.33 with Figure 4.34-4.35 we can conclude that the optimization of the overlay receiver has significant impact on the system performance.

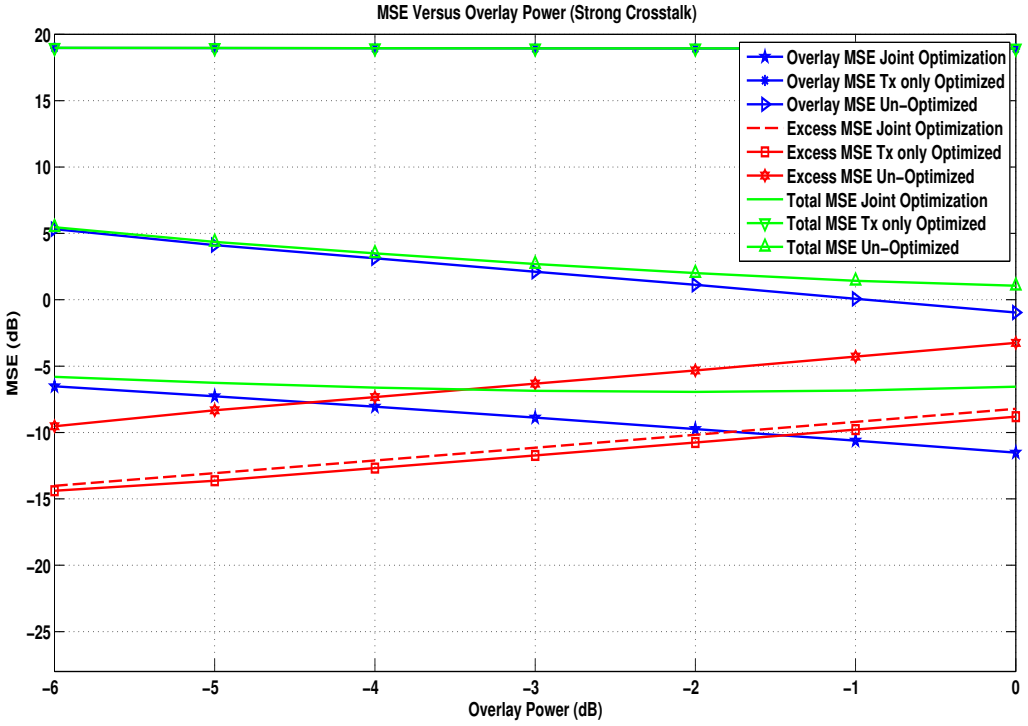

Figure 4.32: Performance loss due to transmitter-only optimization in Case 1.

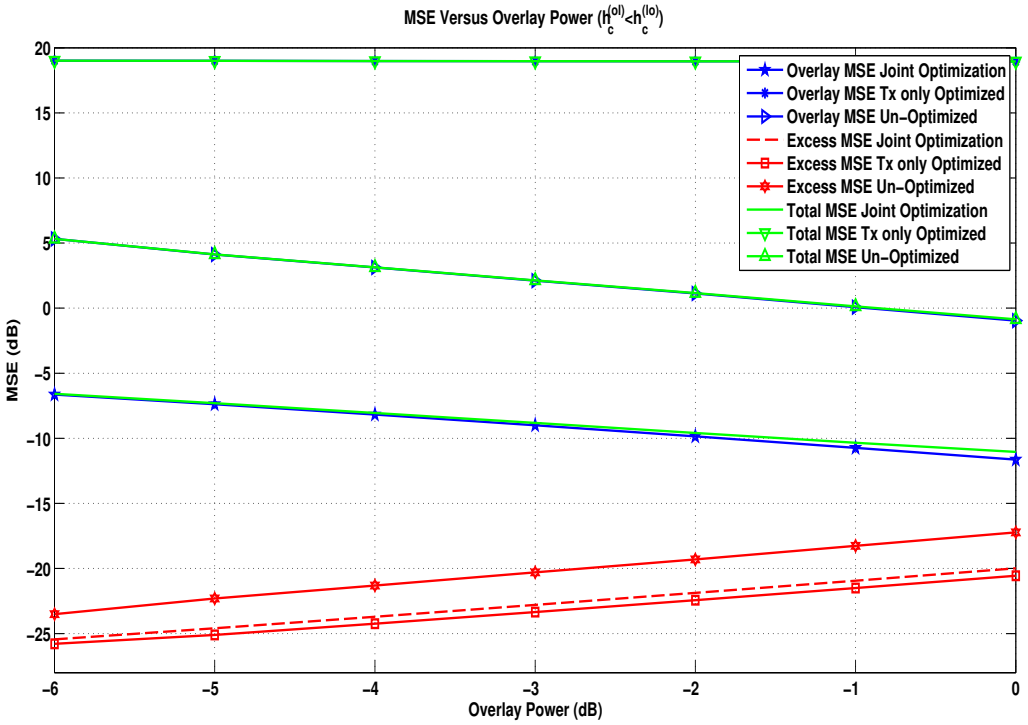

Figure 4.33: Performance loss due to transmitter-only optimization in Case 3.

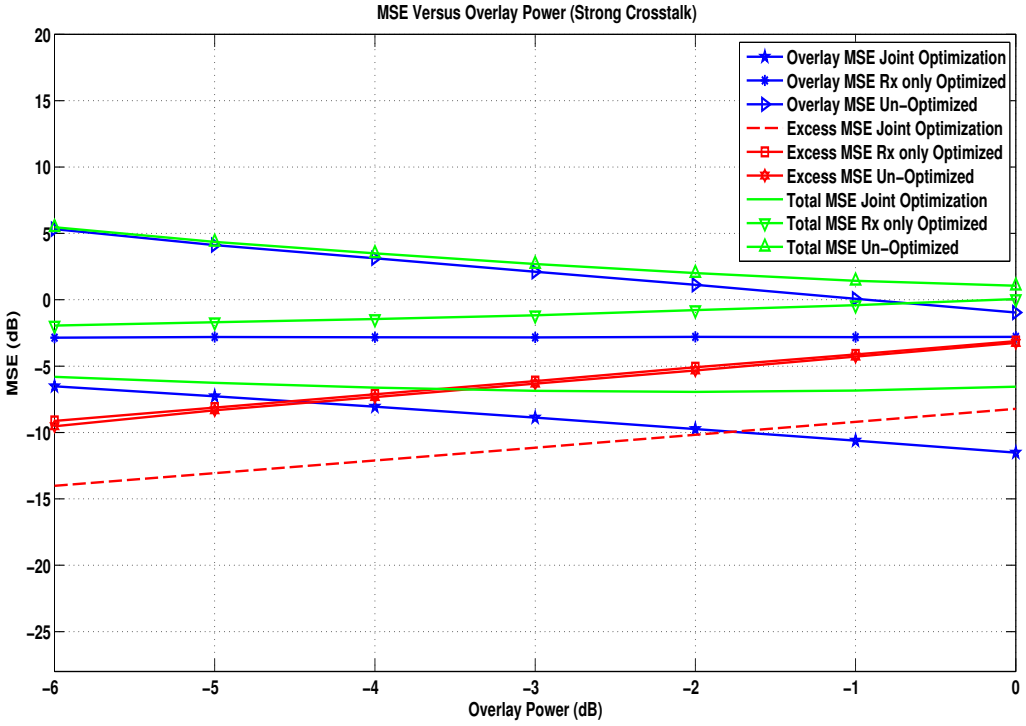

Figure 4.34: Performance loss due to receiver-only optimization in Case 1.

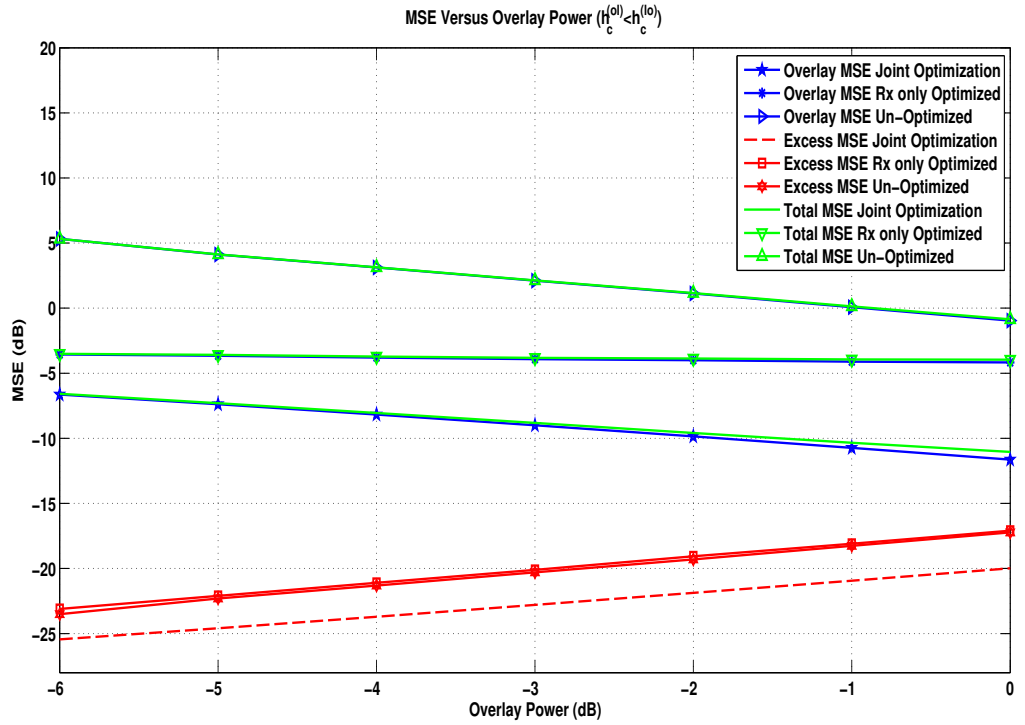

Figure 4.35: Performance loss due to receiver-only optimization in Case 3.

4.1.5 ber performance.

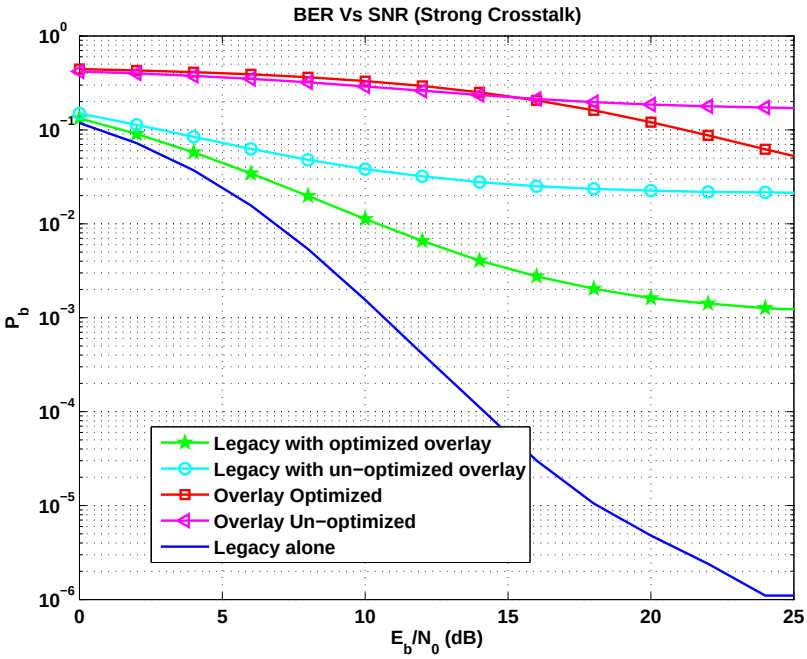

Figure 4.36: BER performance of the optimized and un-optimized systems for Case 1.

Figure 4.36–4.39 implement the Monte Carlo simulation using BPSK (binary phase shift keying) modulation to assess the BER performance of the legacy system in the absence of the overlay system (no crosstalk), the legacy system in the presence of the overlay system, and the overlay system, under different channel conditions. The legacy system was designed to perform optimally in an interference-free environment under the MSE criterion. As such, it is assumed that the legacy system has the requisite channel knowledge to jointly optimize its transmitter and receiver in order to equalize the composite transfer function and combat the effects of fading. Thus, its performance exceeds that of the conventional matched filter architecture. As we see, increasing the SNR improves the performance of both the legacy and the overlay systems. Moreover, when the legacy system is under strong crosstalk (Figure 4.36-4.37), the optimized system performs much better than the un-optimized one and when it is under weak interference (Figure4.38-4.39), the legacy system performs the same as the single user system without the presence of the overlay

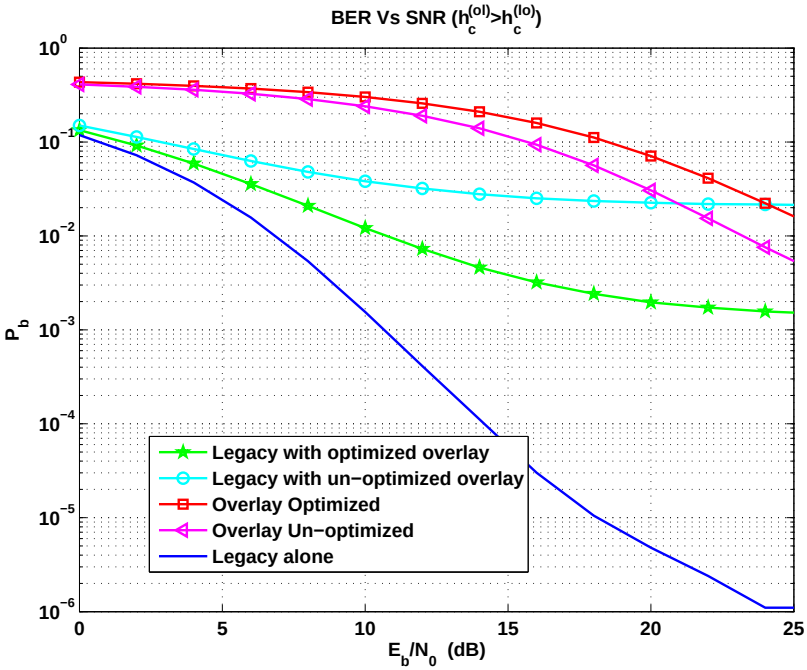

Figure 4.37: BER performance of the optimized and un-optimized systems for Case 2.

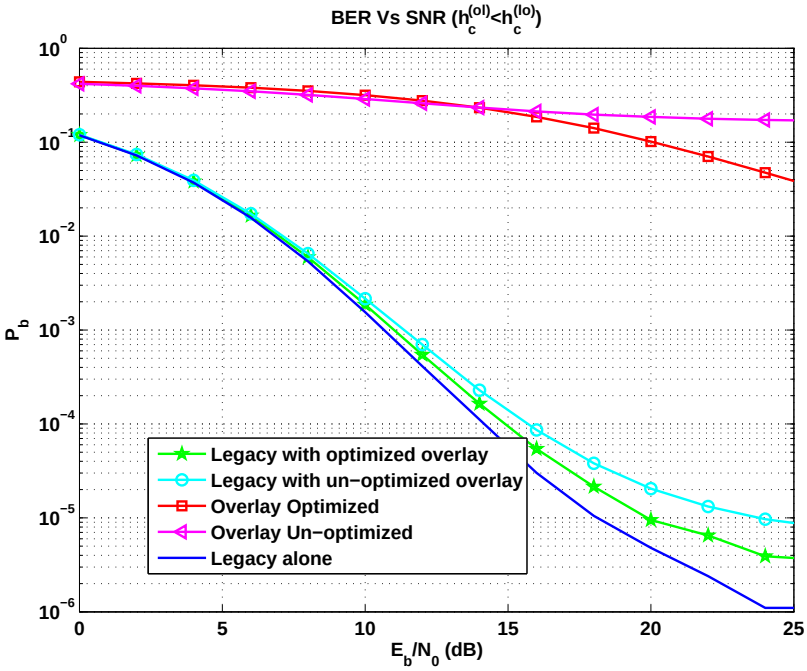

Figure 4.38: BER performance of the optimized and un-optimized systems for Case 3.

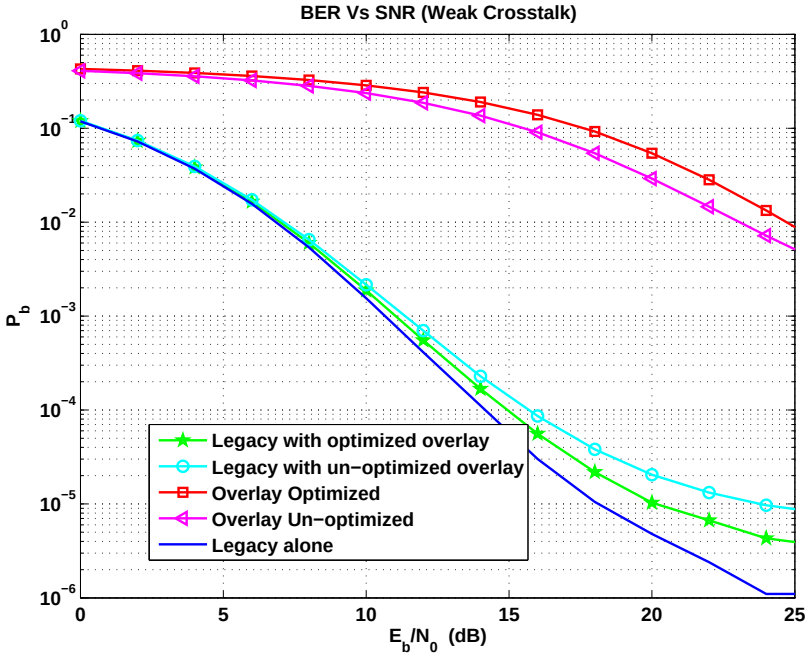

Figure 4.39: BER performance of the optimized and un-optimized systems for Case 4.

system. Additionally, when the overlay system is under more crosstalk (Figure 4.36–4.38), the optimized overlay system performs better than the un-optimized one for an SNR value of 16 dB or above.

It can be seen from Figure 4.36–4.39 that the BER achieved by the optimized overlay system is at a relatively high level. Still, it should be noted that a significant reduction in the BER of the legacy system is achieved through the proposed optimization procedure.

4.2 Dual-Transmit-Antenna System

In this section, we compare the performance of a system having a dual-transmit-antenna overlay with a system having a single-transmit-antenna overlay for different channel conditions, Case 1–4. In Case 2 and Case 3, h_c^{ol} implies the both overlay to legacy crosstalk channels ($h_c^{o_1 l}$ and $h_c^{o_2 l}$).

In Figure 4.40–4.43 we show the variation of the MSE with the overlay transmitter power for both the dual-transmit-antenna and single-transmit-antenna systems when both

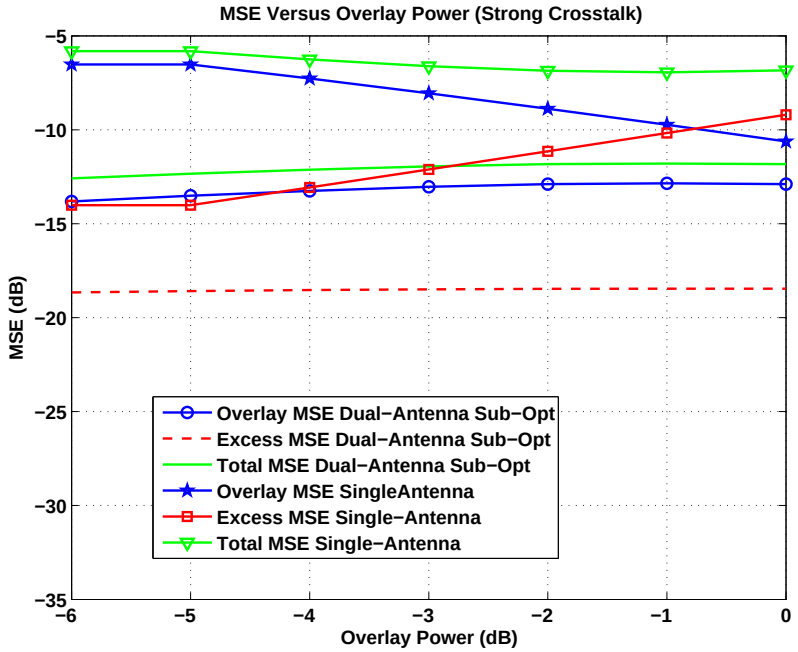

Figure 4.40: Effect of varying overlay power in a system with sub-optimum dual transmit antenna overlay, and a system with single antenna overlay for Case 1.

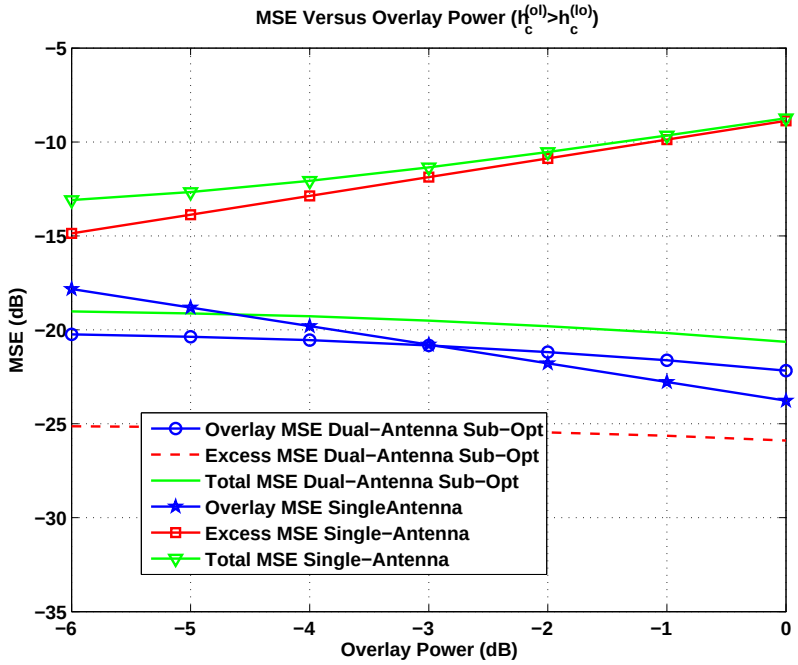

Figure 4.41: Effect of varying overlay power in a system with sub-optimum dual transmit antenna overlay, and a system with single antenna overlay for Case 2.

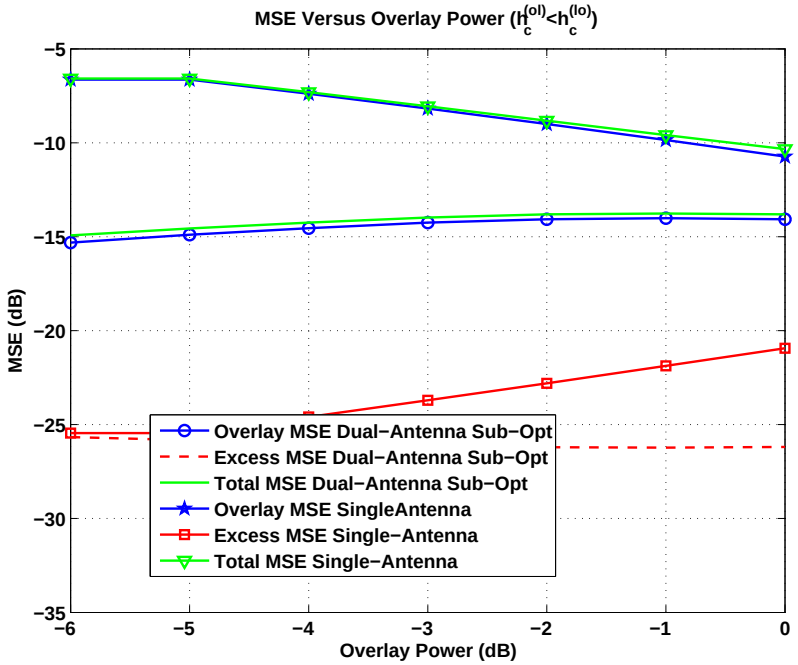

Figure 4.42: Effect of varying overlay power in a system with sub-optimum dual transmit antenna overlay, and a system with single antenna overlay for Case 3.

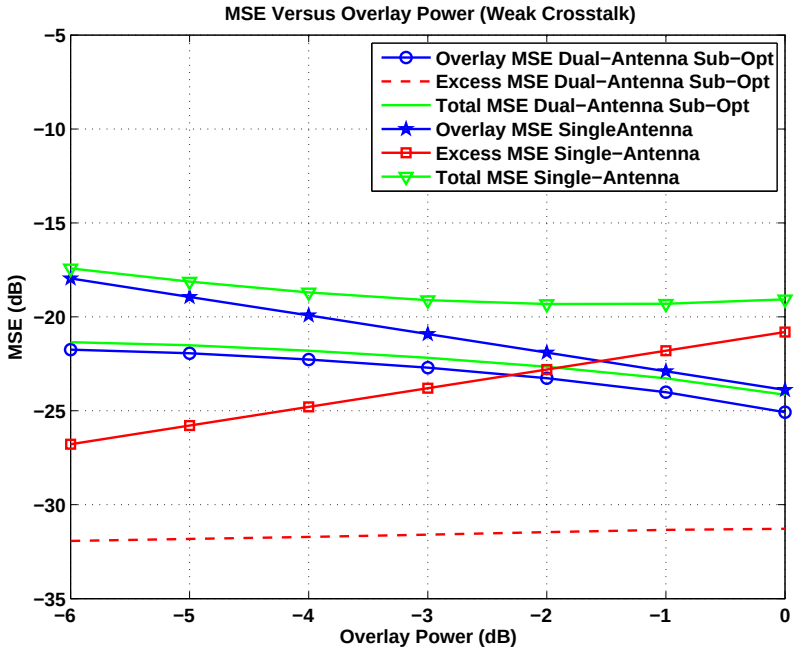

Figure 4.43: Effect of varying overlay power in a system with sub-optimum dual transmit antenna overlay, and a system with single antenna overlay for Case 4.

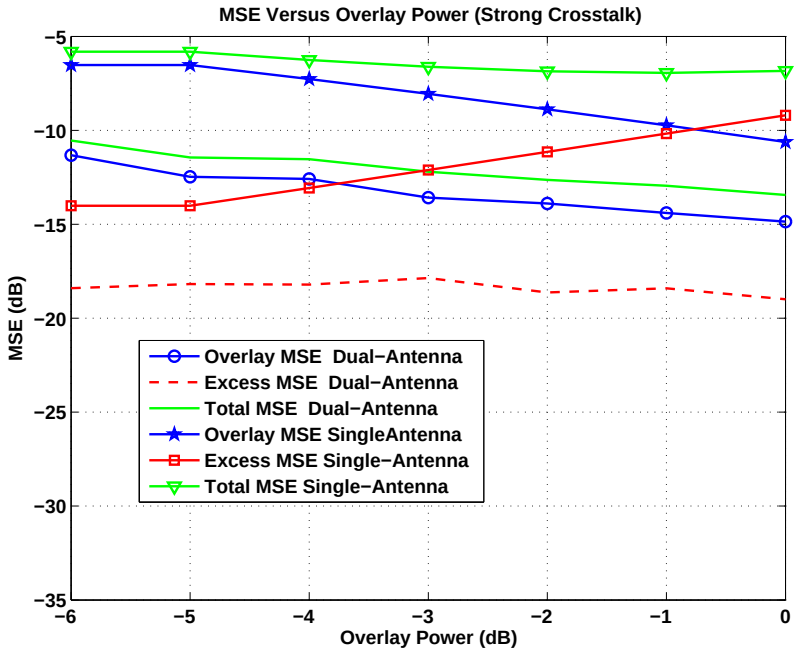

Figure 4.44: Effect of varying overlay power in a system with optimum dual transmit antenna overlay, and a system with single antenna overlay for Case 1.

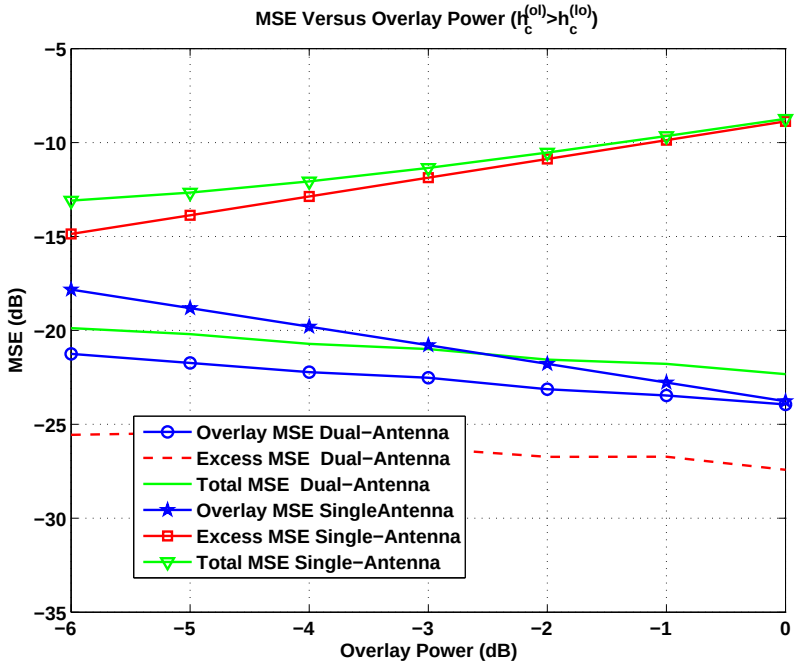

Figure 4.45: Effect of varying overlay power in a system with optimum dual transmit antenna overlay, and a system with single antenna overlay for Case 2.

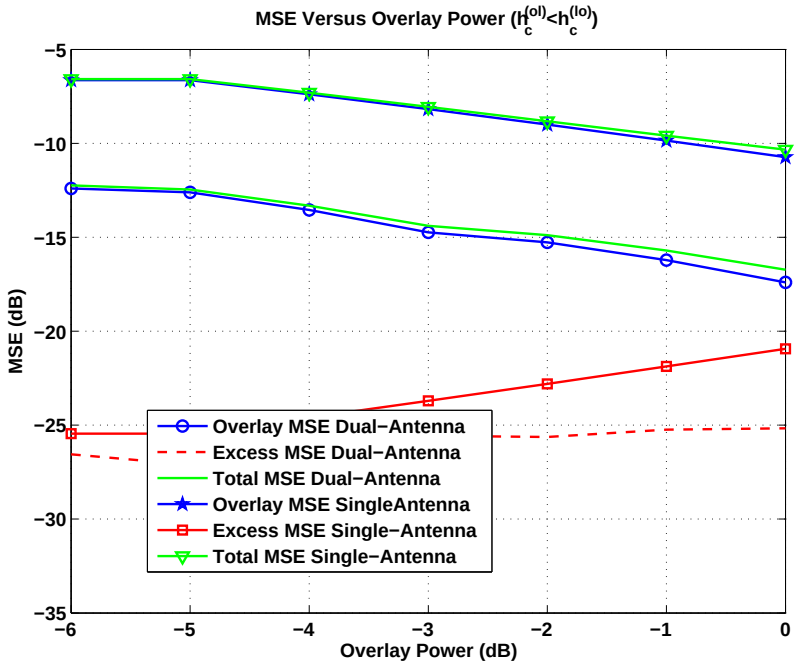

Figure 4.46: Effect of varying overlay power in a system with optimum dual transmit antenna overlay, and a system with single antenna overlay for Case 3.

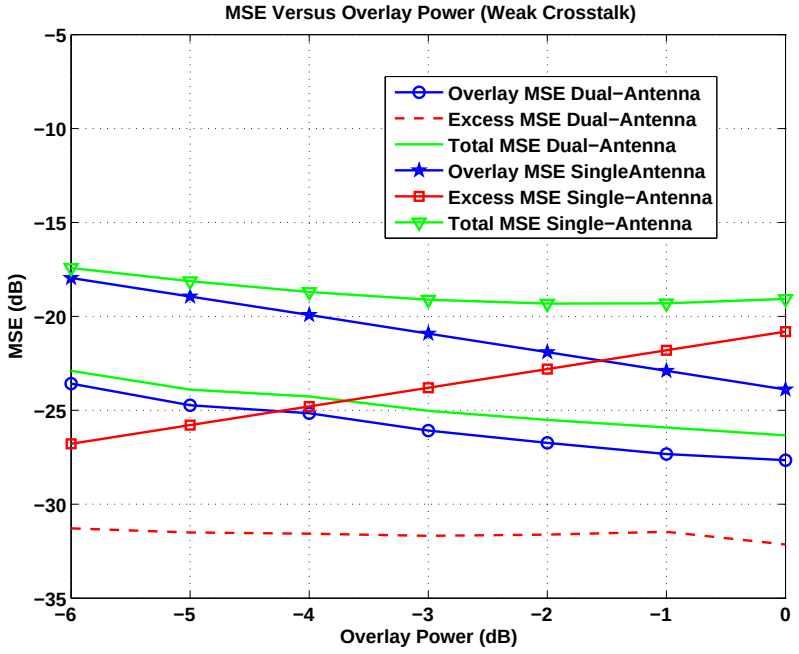

Figure 4.47: Effect of varying overlay power in a system with optimum dual transmit antenna overlay, and a system with single antenna overlay for Case 4.

the legacy and the overlay are completely overlapped in the first Nyquist zone, and $\beta = 1$. For the case of dual-transmit-antenna, the overlay transmitter power is the total available power at the overlay transmitter, which will be allocated to each of the overlay transmitters by sequentially optimizing the Lagrange multipliers, λ_1 and λ_2, in (3.41). As we see, under different crosstalk conditions, the overall performance of the dual-transmit-antenna system is better compared to the single-transmit-antenna one. However, due to the sequential optimization, which is considered to be a sub-optimal solution, the dual-transmit-antenna overlay MSE does not decrease as expected.

It may be noted in Figure 4.40–4.43 that the dual-transmit-antenna overlay MSE does not decrease as expected. Additionally, in Figure 4.41, the single-transmit-antenna overlay MSE is actually lower than the dual-transmit-antenna overlay MSE (the total MSE, however, for the single-transmit-antenna case is always higher than the dual-transmit-antenna case). These effects can be attributed to the sub-optimal sequential optimization procedure that was employed. Indeed, these effects are not observed when a global optimization procedure is used, as will be discussed next.

The overlay, excess, and the total MSEs for the case of jointly optimizing the Lagrange multipliers, λ_1 and λ_2, in (3.41) as a function of the overlay transmitter power are shown in Figure 4.44–4.47. We observe that under different crosstalk conditions, the dual-transmit-antenna system has an MSE that is at least 6 dB less than the single-transmit-antenna case. Moreover, unlike the sequential optimization case (Figure 4.40–4.43), increasing the overlay power improves the overlay system performance. Therefore, joint optimization of the Lagrange multipliers results in an optimum solution but it is more computationally complex.

Chapter 5

Conclusion

Cognitive radio, a recently developed technology, is a highly flexible alternative to the conventional single frequency band wireless devices, which allows sharing the spectrum between the existing and the new systems. The task of spectrum sensing is one of the most crucial components in the establishment of the cognitive radio. In this thesis, a wireless communication network was addressed whereby an overlay system can operate simultaneously in the same frequency band as the legacy user over a flat Rayleigh fading channel without the need of spectrum sensing. The overlay user's transmitter/receiver responses are computed in a manner that optimizes self-performance while mitigating the interference introduced to the legacy user. A weighted sum of the MSE of the new system plus the excess MSE in the existing system due to the introduction of the overlay system was used as a figure of merit.

The performance of the optimized system compared to an un-optimized one (when the transmitter and receiver of the overlay system are simply matched filters) was assessed in terms of MSE and BER. It was shown that using the optimized single-transmit-antenna overlay system can generally yield to a 10 dB improvement in the system MSE. The system was then extended to a dual-transmit-antenna system. Simulation results indicate a further 6 dB gain in the system MSE using dual-transmit-antenna overlay.

The sensitivity of the system to accuracy of the SNR estimate and the channel estimate was also examined. It was shown that the system can still work even in the case of an inaccurate SNR and channel estimations. In addition, to reduce the complexity, a

system having a fixed transmitter or receiver pulse shape was studied. It was observed that the legacy excess MSE is fairly insensitive to the transmitter-only optimization. However, optimizing the overlay transmitter only leads to a significant degradation of the overlay system performance. On the other hand, the overall system performance in the case of the receiver-only optimization is between the joint optimization and the un-optimized case. Thus, optimizing only the receiver of the overlay system leads to a suboptimal solution.

The current work can be extended in a multitude of ways:

- The usage of higher-order modulation schemes can be investigated in order to further improve the spectral efficiency. In a similar vein, a scenario in which a spread spectrum overlay system is employed can be studied, along with tradeoffs such as interference level at the legacy system and the data rate supported by the overlay system.

- The current work has tackled the problem of cognitive radio system in the context of coexistence between the overlay system and the legacy system when both operate over a flat Rayleigh fading channel. This problem can also be tackled for the case when the systems operate over a multi-path fading channel.

- In the case of dual-transmit-antennas, we have assumed that the same data streams are fed to both overlay transmitters which leads to some diversity gain. However, the capacity of the system can be increased by feeding different data streams into each overlay transmitter. The proposed dual-transmit-antenna system can be extended to a system having multiple transmit/receive antennas.

- The present simulation deals only with scenarios where the overlay user shares the same bandwidth with one legacy user; an optimum transmitter/receiver for an overlay system that shares the same bandwidth with multiple legacy systems can be investigated. In such scenarios, the scalability of the proposed architecture can be examined vis-a-vis using other techniques such as cooperative spectrum sensing.

- An important practical issue is how channel estimation will be performed at the overlay transmitter/reciever. As such, further study can be conducted to determine the requirements of the feedback architecture needed to obtain the necessary channel estimates.

References

[1] H. Mir and S. Roy, "Optimum transmitter/receiver design for a narrowband overlay in noncoordinated subscriber lines," *Communications, IEEE Transactions on*, vol. 52, no. 6, pp. 992-998, June 2004.

[2] B. Wang and K. Ray Liu, "Advances in cognitive radio networks: A survey," *IEEE Journal of Selected Topics in Signal Processing*, vol. 5, no. 1, February 2011.

[3] N. Devroye, P. Mitran, and V. Tarokh, "Limits on communications in a cognitive radio channel," *IEEE Communication Magazine*, June 2006.

[4] F. Akyildiz, W. Lee, M. Vuran, and S. Mohanty, "Next generation/dynamic spectrum access/cognitive radio wireless networks: A survey," *Computer Networks*, vol. 50, pp. 2127-2159, May 2006.

[5] T. Yucek and H. Arslan, "A Survey of spectrum sensing algorithms for cognitive radio application," *IEEE Communications Surveys Tutorials*, vol. 11, no. 1, 2009.

[6] J. Mitola,"Cognitive Radio: making software radio more personal," *Personal Communications, IEEE*, Vol. 06, No. 04, pp. 48-52, Aug.1999.

[7] S. Haykin, "Cognitive radio: Brain-empowered wireless communications," *Selected Areas in Communications, IEEE Journal on*, vol. 23, no. 2, pp. 201-220, Feb. 2005.

[8] M. Gandetto, A. Cattoni, and C. Regazzoni, "A distributed approach to mode identification and spectrum monitoring for cognitive radios," *in Proc. SDR Forum Technical Conference*, Orange County, California, USA, Nov. 2005.

[9] N. Devroye,"Information theoretical limits on cognitive radio networks," *Cognitive Radio Communications and Networks; Principles and Practice*, A. Wyglinski, M. Nekovee and Y. T. Hou Ed., Elsevier, 2009.

[10] C. Raman, R. Yates, N. Mandayam, "Scheduling variable rate links via a spectrum server," *New Frontiers in Dynamic Spectrum Access Networks. 2005 First IEEE International Symposium on*, vol., no., pp.110-118, 8-11 Nov. 2005.

[11] D. Cabric, S. Mishra, and R. Brodersen, "Implementation issues in spectrum sensing for cognitive radios," *Signals, Systems and Computers, 2004. Conference Record of the Thirty-Eighth Asilomar Conference on*, vol.1, no., pp. 772- 776 Vol.1, 7-10 Nov. 2004.

[12] A. Ghasemi and E. Sousa, "Collaborative spectrum sensing for opportunistic access in fading environments," *New Frontiers in Dynamic Spectrum Access Networks. 2005 First IEEE International Symposium on* , vol., no., pp.131-136, 8-11 Nov. 2005.

[13] H. Tang, "Some physical layer issues of wide-band cognitive radio systems," *New Frontiers in Dynamic Spectrum Access Networks. 2005 First IEEE International Symposium on*, vol., no., pp.151-159, 8-11 Nov. 2005.

[14] S. Shankar, C. Cordeiro, K. Challapali, "Spectrum agile radios: utilization and sensing architectures," *New Frontiers in Dynamic Spectrum Access Networks. 2005 First IEEE International Symposium on*, vol., no., pp.160-169, 8-11 Nov. 2005.

[15] A. Molisch, L. Greenstein, and M. Shafi, "Propagation issues for cognitive radio," *Proceedings of the IEEE*, vol.97, no.5, pp.787-804, May 2009.

[16] C. Sun, Y. Alemseged, H. Tran, and H. Harada, "Transmit power control for cognitive radio over a Rayleigh fading channel," *Vehicular Technology, IEEE Transactions on*, vol.59, no.4, pp.1847-1857, May 2010.

[17] W. Jiang and H. Ma, "Cooperative spectrum sensing for sognitive radio in Rayleigh channels," *Information Science and Engineering (ICISE), 2009 1st International Conference on*, vol., no., pp.2595-2598, 26-28 Dec. 2009.

[18] Y. Li, Y. Zhang, and H. Zhang, "Primary signal detection over Rayleigh fading channel for cognitive radio," *Uncertainty Reasoning and Knowledge Engineering (URKE), 2011 International Conference on*, vol.1, no., pp.239-242, 4-7 Aug. 2011.

[19] S. Nallagonda, S. Roy, and S. Kundu, "Performance of cooperative spectrum sensing with censoring of cognitive radios in Rayleigh fading channel," *India Conference (INDICON), 2011 Annual IEEE*, vol., no., pp.1-5, 16-18 Dec. 2011.

[20] S. Nallagonda, S. Roy, and S. Kundu, "Cooperative spectrum sensing with censoring of cognitive radios in Rayleigh fading channel," *Communications (NCC), 2012 National Conference on*, vol., no., pp.1-5, 3-5 Feb. 2012.

[21] M. Mohammadkarimi, B. Mahboobi, and M. Ardebilipour, "Optimal spectrum sensing in fast fading Rayleigh channel for cognitive radio," *Communications Letters, IEEE*, vol.15, no.10, pp.1032-1034, October 2011.

[22] H. Vu, T. Duy, and H. Kong, "An optimal cooperative spectrum sensing method in cognitive radio network over Rayleigh fading channel," *Wireless Days (WD), 2011 IFIP*, vol., no., pp.1-5, 10-12 Oct. 2011.

[23] H. Mir, "Optimum transmitter/receiver design in an overlay system," *Engineering Systems Management and Its Applications (ICESMA), 2010 Second International Conference on*, vol., no., pp.1-4, March 30 2010-April 1 2010.

[24] Y. Xiaogeng, O. Muta, and Y. Akaiwa, "Iterative joint optimization of transmit/receive frequency-domain equalization in single carrier wireless communication systems," *Vehicular Technology Conference, 2008. VTC 2008-Fall. IEEE 68th* , vol., no., pp.1-5, 21-24 Sept. 2008.

[25] P. Kumar and S. Roy, "Optimization for crosstalk suppression with noncoordinating users," *Communications, IEEE Transactions on*, vol. 44, pp. 894-905, July 1996.

[26] J. Cho, "Joint transmitter and receiver optimization in additive cyclostationary noise," *Information Theory, IEEE Transactions on*, vol. 50, no. 14, pp. 3396-3405, Dec. 2004.

[27] Y. Yun and J. Cho, "A design of optimal overlay system inducing zero interference to legacy systems," *Global Telecommunications Conference* ,vol., no., pp.1462-1466, 26-30Nov. 2007.

[28] Y. Yun and J. Cho, "An optimal orthogonal overlay for a cyclostationary legacy signal," *Communications, IEEE Transactions on*, vol. 58, no. 5, pp. 1557-1567, May 2010.

[29] H. Sampath and A. Paulraj, "Joint transmit and receive optimization for high data rate wireless communication using multiple antennas," *Signals, Systems, and Computers, 1999. Conference Record of the Thirty-Third Asilomar Conference on* , vol.1, no., pp.215-219, 1999.

[30] T. Bogale and L. Vandendorpe, "Robust sum MSE optimization for downlink multiuser MIMO systems with arbitrary power constraint: Generalized duality approach," *Signal Processing, IEEE Transactions on*, vol.60, no.4, pp.1862-1875, April 2012.

[31] S. Serbetli and A. Yener, "Transceiver optimization for multiuser MIMO systems," *Signal Processing, IEEE Transactions on*, vol.52, no.1, pp. 214- 226, Jan. 2004.

[32] E. Jorswieck and H. Boche, "Transmission strategies for the MIMO MAC with MMSE receiver: average MSE optimization and achievable individual MSE region," *Signal Processing, IEEE Transactions on*, vol. 51, no. 11, pp. 28722881, Nov. 2003.

[33] X. Gong, M. Jordan, A. Ishaque, G. Dartmann, G. Ascheid, "Robust MSE-Based transceiver optimization in MISO downlink cognitive radio network," *Wireless Communications and Networking Conference (WCNC), 2010 IEEE*, vol., no., pp.1-6, 18-21 April 2010.

[34] X. Gong, A. Ishaque, G. Dartmann, and G. Ascheid, "MSE-based linear transceiver optimization in MIMO cognitive radio networks with imperfect channel knowledge," *Cognitive Information Processing (CIP), 2010 2nd International Workshop on* , vol., no., pp.105-110, 14-16 June 2010.

[35] B. Seo, "Joint design of precoder and receiver in cognitive radio networks using an MSE criterion," *Signal Processing*, vol. 91, no. 11, pp. 2623-2629, 2011.

[36] L. Le and H. Ekram, "Resource allocation for spectrum underlay in cognitive radio networks," *Wireless Communications, IEEE Transactions on* , vol.7, no.12, pp.5306-5315, December 2008.

[37] M. Vameghestahbanati, H. Mir, and M. El-Tarhuni, "Joint transmitter/receiver optimization for overlay wireless systems," *Wirelss Telecommunications Symposium (WTS), 2012*, vol., no., pp.1-5, 18-20 April 2012.

Appendix A
Derivation of Frequency Domain Expression for MSE

In this section, we present the derivation for the frequency domain expression for composite mean square error. The derivation is given in the context of the dual-transmit-antenna case for the sake of generality, since it subsumes the single-antenna-case.

Given the constraint that the legacy system is fixed and cannot be modified, a composite MSE is given by

$$MSE = MSE_1 + \beta MSE_2^e \tag{A.1}$$

$$\begin{aligned} MSE_1 &\equiv \text{MSE in channel 1 (overlay MSE)} \\ &= E\left[|z_{1n} - \hat{z}_{1n}|^2\right] \end{aligned} \tag{A.2}$$

$$\begin{aligned} MSE_2^e &= \text{legacy excess MSE} \\ &= E\left[|q_{2n}|^2\right] \end{aligned} \tag{A.3}$$

and where

$$q_{2n} \triangleq q_2(t)\Big|_{t=nT} \tag{A.4}$$

$$q_2(t) = \left[h_t^{(o_1)}(t) * h_c^{(o_1 l)}(t) + h_t^{(o_2)}(t) * h_c^{(o_2 l)}(t)\right] * h_r^{(l)}(t) \tag{A.5}$$

where $*$ denotes the convolution and $h_t^{(o_1)}(t) \leftrightarrow H_t^{(o_1)}(f)$, $h_t^{(l)}(t) \leftrightarrow H_t^{(l)}(f)$ form a Fourier transform pair and $h_t^{(o_1)}(t)$, $h_t^{(l)}(t)$ indicate the pulse shaping at the corresponding point in the transmitters and the same notations are used for channel and receiver.

Moreover, MSE_2^e in $(A.3)$ represents the imposed excess MSE into the legacy system by introducing the overlay system. Furthermore, β is a weighting in the optimization problem between MSE_1 and MSE_2^e and can be selected to weight or de-weight MSE_2^e by using large value or small value of β.

The output signals $x_1(t)$ and $x_2(t)$ are produced by processing the signal at the receiver input in the presence of AWGN $w_1(t)$ and $w_2(t)$ through the receiver filters $h_r^{(o)}(t)$ and $h_r^{(l)}(t)$ and are the input to the decision device (which is actually a sampler followed by a threshold comparison) to generate the final estimates,

$$\begin{aligned} x_1(t) &= \sum_{n=-\infty}^{\infty} z_{1n} p_{11}(t-nT) \\ &\quad + \sum_{n=-\infty}^{\infty} z_{2n} p_{21}(t-nT) + \upsilon_1(t) \end{aligned} \tag{A.6}$$

$$\upsilon_1(t) = w_1(t) * h_r^{(o)}(t) \tag{A.7}$$

$$S_{\upsilon_1} = N_0 \left| H_r^{(o)}(f) \right|^2 \tag{A.8}$$

where S_{υ_1} denotes the power spectral density of $\upsilon_1(t)$, and

$$p_{11}(t) = \left[h_t^{(o_1)}(t) * h_c^{(o_1 o)}(t) + h_t^{(o_2)}(t) * h_c^{(o_2 o)}(t) \right] * h_r^{(o)}(t) \tag{A.9}$$

$$p_{21}(t) = h_t^{(l)}(t) * h_c^{(lo)}(t) * h_r^{(o)}(t) \tag{A.10}$$

It is assumed that both the overlay and the legacy systems have the same bandwidth $1 \setminus T$, where T denotes the symbol period.

It is assumed that $x_1(t)$ is synchronously sampled at instants nT; the sample at instant $t = 0$ is represented by x_{10} and σ^2 denotes the input symbol variance; also, N_0 is the additive noise power spectral density. Then

$$
\begin{aligned}
x_{10} &= \sum_{n=-\infty}^{\infty} z_{1n} p_{11}\left(nT\right) \\
&\quad + \sum_{n=-\infty}^{\infty} z_{2n} p_{21}\left(nT\right) + \upsilon_{10}
\end{aligned} \tag{A.11}
$$

$$
E\left[\left|x_{10} - z_{10}\right|^2\right] = E\left[\left|a - b\right|^2\right] \tag{A.12}
$$

where

$$
\begin{aligned}
a &= \alpha^2 + \beta^2 + \gamma^2 \\
\alpha &= \sum_{n=-\infty}^{\infty} z_{1n} p_{11}\left(nT\right) \\
\beta &= \sum_{n=-\infty}^{\infty} z_{2n} p_{21}\left(nT\right) \\
\gamma &= \upsilon_{10}
\end{aligned} \tag{A.13}
$$

and

$$
b = z_{10} \tag{A.14}
$$

$$
\left\langle \left|a - b\right|^2 \right\rangle = \left\langle a^2 \right\rangle + \left\langle b^2 \right\rangle - 2\left\langle ab \right\rangle \tag{A.15}
$$

$$
\begin{aligned}
a^2 &= \left(\alpha + \beta + \gamma\right)^2 \\
&= \left(\alpha + \beta\right)^2 + \gamma^2 + 2\gamma\left(\alpha + \beta\right)
\end{aligned} \tag{A.16}
$$

Since noise is uncorrelated with both the legacy and the overlay data, and the legacy and the overlay data are uncorrelated with each other

$$
a^2 = \alpha^2 + \beta^2 + \gamma^2 \tag{A.17}
$$

Therefore

$$\left\langle a^2 \right\rangle = \left\langle \alpha^2 + \beta^2 + \gamma^2 \right\rangle \tag{A.18}$$

$$\left\langle \alpha^2 \right\rangle = \sum_n \sum_k \underbrace{\left\langle z_{1n}\ z_{1k} \right\rangle}_{\sigma^2 \delta_{nk}} p_{11}\left(nT\right) p_{11}\left(kT\right) = \sum_n \sigma^2 p_{11}^2\left(nT\right) \tag{A.19}$$

$$\left\langle \beta^2 \right\rangle = \sum_n \sum_k \underbrace{\left\langle z_{2n}\ z_{2k} \right\rangle}_{\sigma^2 \delta_{nk}} p_{21}\left(nT\right) p_{21}\left(kT\right) = \sum_n \sigma^2 p_{21}^2\left(nT\right) \tag{A.20}$$

$$\left\langle \gamma^2 \right\rangle = N_0 \int \left|\upsilon_{10}\right|^2 dt \tag{A.21}$$

Substituting $(A.19)$–$(A.21)$ into $(A.18)$

$$\left\langle a^2 \right\rangle = \sum_n \sigma^2 p_{11}^2\left(nT\right) + \sum_n \sigma^2 p_{21}^2\left(nT\right) + N_0 \int \left|\upsilon_{10}\right|^2 dt \tag{A.22}$$

$$\left\langle b^2 \right\rangle = \left\langle z_{10}^2 \right\rangle = \sigma^2 \delta_{n0} \tag{A.23}$$

$$\begin{aligned} \left\langle ab \right\rangle &= \left\langle \alpha^2 b + \beta^2 b + \gamma^2 b \right\rangle = \left\langle \alpha^2 b \right\rangle \\ &= \sum_n \underbrace{\left\langle z_{1n}\ z_{10} \right\rangle}_{\sigma^2 \delta_{n0}} p_{11}^2\left(nT\right) = \sigma^2 p_{11}^2\left(0\right) \end{aligned} \tag{A.24}$$

Substituting $(A.22)$–$(A.24)$ into $(A.15)$

$$\begin{aligned} E\left[\left|x_{10} - Z_{10}\right|^2\right] &= \left\langle \left|a - b\right|^2 \right\rangle \\ &= \sigma^2 \left\{ \sum_n \left[p_{11}^2\left(nT\right) + p_{21}^2\left(nT\right) \right] + \delta_{n0} - 2p_{11}^2\left(0\right) \right\} \\ &\quad + N_0 \int \left|\upsilon_{10}\right|^2 dt \end{aligned} \tag{A.25}$$

where

$$\begin{aligned}\sigma^2 \sum_n p_{11}^2 (nT) + \delta_{n0} - 2p_{11}^2 (0) &= \sigma^2 \sum_n p_{11}^2 (nT) + \delta_{n0} - 2\delta_{n0} p_{11}^2 (nT) \\ &= \sigma^2 \sum_{n=-\infty}^{\infty} |p_{11} (nT) - \delta_{n0}|^2 \end{aligned} \quad (A.26)$$

Then

$$\begin{aligned}E\left[|x_{10} - Z_{10}|^2\right] &= \sigma^2 \sum_{n=-\infty}^{\infty} |p_{11} (nT) - \delta_{n0}|^2 \\ &\quad + \sigma^2 \sum_n |p_{21} (nT)|^2 \\ &\quad + N_0 \int |\upsilon_{10}|^2 dt \end{aligned} \quad (A.27)$$

Applying Parseval's theorem on $(A.7)$–$(A.10)$ and substituting in $(A.27)$

$$\begin{aligned}MSE_1 &= E\left[|x_{10} - Z_{10}|^2\right] \\ &= \frac{\sigma^2}{T} \int_{-\frac{1}{2T}}^{\frac{1}{2T}} \left| \left[H_t^{(o_1)} (f) H_c^{(o_1 o)} (f) + H_t^{(o_2)} (f) H_c^{(o_2 o)} (f) \right] H_r^{(o)} (f) - T \right|^2 \\ &\quad + \frac{\sigma^2}{T} \int_{-\frac{1}{2T}}^{\frac{1}{2T}} \left| H_t^{(l)} (f) H_c^{(lo)} (f) H_r^{(o)} (f) \right|^2 df \\ &\quad + N_0 \int_{-\frac{1}{2T}}^{\frac{1}{2T}} \left| H_r^{(o)} (f) \right|^2 df \end{aligned} \quad (A.28)$$

Applying similar procedures on $(A.5)$

$$MSE_2^e = \frac{\sigma^2}{T} \int_{-\frac{1}{2T}}^{\frac{1}{2T}} \left| \left[H_t^{(o_1)} (f) H_c^{(o_1 l)} (f) + H_t^{(o_2)} (f) H_c^{(o_2 l)} (f) \right] H_r^{(l)} (f) \right|^2 df \quad (A.29)$$

The average transmitter power on the overlay user is

$$P_t = \frac{\sigma^2}{T} \int_{-\frac{1}{2T}}^{\frac{1}{2T}} \left(\left| H_t^{(o_1)} (f) \right|^2 + \left| H_t^{(o_2)} (f) \right|^2 \right) df \quad (A.30)$$

The optimization problem of optimizing $(A.1)$ subject to the average power constraint in $(A.30)$ can be rewritten as below by introducing a Lagrange multiplier λ

$$MSE = MSE_1 + \beta MSE_2^e + \lambda P_t \tag{A.31}$$

Substituting $(A.28)$–$(A.30)$ into $(A.31)$

$$\begin{aligned} MSE \;=\; & \frac{\sigma^2}{T}\int_{-\frac{1}{2T}}^{\frac{1}{2T}} \left|\left[H_t^{(o_1)}(f)\,H_c^{(o_1 o)}(f) + H_t^{(o_2)}(f)\,H_c^{(o_2 o)}(f)\right] H_r^{(o)}(f) - T\right|^2 \\ & + \frac{\sigma^2}{T}\int_{-\frac{1}{2T}}^{\frac{1}{2T}} \left|H_t^{(l)}(f)\,H_c^{(lo)}(f)\,H_r^{(o)}(f)\right|^2 df \\ & + N_0\int_{-\frac{1}{2T}}^{\frac{1}{2T}} \left|H_r^{(o)}(f)\right|^2 df \\ & + \beta\frac{\sigma^2}{T}\int_{-\frac{1}{2T}}^{\frac{1}{2T}} \left|\left[H_t^{(o_1)}(f)\,H_c^{(o_1 l)}(f) + H_t^{(o_2)}(f)\,H_c^{(o_2 l)}(f)\right] H_r^{(l)}(f)\right|^2 df \\ & + \lambda\frac{\sigma^2}{T}\int_{-\frac{1}{2T}}^{\frac{1}{2T}} \left(\left|H_t^{(o_1)}(f)\right|^2 + \left|H_t^{(o_2)}(f)\right|^2\right) df \end{aligned} \tag{A.32}$$

Appendix B
Optimum Derivation for Single-Transmit-Antenna system

By setting the derivative of (3.14) with respect to $H_t^{(o)}$ and $H_r^{(o)}$ to zero, we arrive at the following:

$$H_r^{(o)}(f) = \frac{TH_t^{(o)}(f)^* H_c^{(oo)}(f)^*}{|H_t^{(o)}(f)|^2 |H_c^{(oo)}(f)|^2 + |H_t^{(l)}(f)|^2 |H_c^{(lo)}(f)|^2 + \eta^{-1}} \tag{A.33}$$

$$H_t^{(o)}(f) = \frac{TH_r^{(o)}(f)^* H_c^{(oo)}(f)^*}{|H_r^{(o)}(f)|^2 |H_c^{(oo)}(f)|^2 + (\beta |H_r^{(l)}(f)|^2 |H_c^{(ol)}(f)|^2 + \lambda)} \tag{A.34}$$

Moreover, by equating the the derivative of (3.14) with respect to $H_t^{(o)}$ and $H_r^{(o)}$, the additional relation is found:

$$\left[\beta |H_r^{(l)}(f)|^2 |H_c^{(ol)}(f)|^2 + \lambda\right] |H_t^{(o)}(f)|^2 = \left[|H_t^{(l)}(f)|^2 |H_c^{(lo)}(f)|^2 + \eta^{-1}\right] |H_r^{(o)}(f)|^2 \tag{A.35}$$

Obtaining $H_r^{(o)}(f)^*$ from (A.33) and substituting in the numerator of (A.34), and simplifying results in

$$\begin{aligned} T^2 |H_c^{(oo)}(f)|^2 \;=\; & \left[|H_c^{(oo)}(f)|^2 |R_1|^2 + (\beta |H_c^{(ol)}(f)|^2 |H_r^{(l)}(f)|^2 + \lambda)\right] \\ & \left[|H_t^{(o)}(f)|^2 |H_c^{(oo)}(f)|^2 + |H_t^{(l)}(f)|^2 |H_c^{(lo)}(f)|^2 + \eta^{-1}\right] \end{aligned} \tag{A.36}$$

Substituting for $|H_t^{(o)}(f)|^2$ from (A.35) as $|H_t^{(o)}(f)|^2 = G|H_r^{(o)}(f)|^2$, where

$$G = \frac{|H_t^{(l)}(f)|^2 |H_c^{(lo)}(f)|^2 + \eta^{-1}}{\beta |H_r^{(l)}(f)|^2 |H_c^{(ol)}(f)|^2 + \lambda} \tag{A.37}$$

gives

$$a|H_r^{(o)}(f)|^4 + b|H_r^{(o)}(f)|^2 + c = 0 \tag{A.38}$$

Appendix C

Optimum Derivation for Dual-Transmit-Antenna system

Taking the derivative of (3.45) with respect to $H_r^{(o)}$

$$\begin{aligned}\frac{\partial MSE}{\partial H_r^{(o)}} &= 2\frac{\sigma^2}{T}\left[\mathbf{H_t^{(o)\intercal}H_c^{(oo)}}\left[\mathbf{H_t^{(o)\intercal}H_c^{(oo)}}H_r^{(o)}-T\right]\right] \\ &\quad + 2\frac{\sigma^2}{T}\left|H_t^{(l)}H_c^{(lo)}\right|^2 H_r^{(o)} \\ &\quad + 2N_0H_r^{(o)} = \mathbf{0} \end{aligned} \tag{A.39}$$

which leads to

$$\left[\mathbf{H_t^{(o)\intercal}H_c^{(oo)}H_t^{(o)\intercal}H_c^{(oo)}} + \left|H_t^{(l)}\right|^2\left|H_c^{(lo)}\right|^2 + \frac{TN_0}{\sigma^2}\right]H_r^{(o)} = T\mathbf{H_t^{(o)\intercal}H_c^{(oo)}} \tag{A.40}$$

Similarly,taking the derivative of (3.45) with respect to $\mathbf{H_t^{(o)}}$

$$\begin{aligned}\frac{\partial MSE}{\partial \mathbf{H_t^{(o)}}} &= 2\frac{\sigma^2}{T}H_r^{(o)}\mathbf{H_c^{(oo)}}\left[\mathbf{H_c^{(oo)\intercal}}H_r^{(o)}\mathbf{H_t^{(o)}}-T\right] \\ &\quad + 2\beta\frac{\sigma^2}{T}\mathbf{H_c^{(ol)}H_c^{(ol)\intercal}H_t^{(o)}}\left|H_r^{(l)}\right|^2 \\ &\quad + 2\frac{\sigma^2}{T}\boldsymbol{\lambda}\mathbf{H_t^{(o)}} = \mathbf{0} \end{aligned} \tag{A.41}$$

which yields to

$$\left[\left|H_r^{(o)}\right|^2\mathbf{H_c^{(oo)}H_c^{(oo)\intercal}} + \beta\left|H_r^{(l)}\right|^2\mathbf{H_c^{(ol)}H_c^{(ol)\intercal}} + \boldsymbol{\lambda}\right]\mathbf{H_t^{(o)}} = TH_r^{(o)}\mathbf{H_c^{(oo)}} \tag{A.42}$$

$(A.40)$ and $(A.42)$ can be written as

$$\mathbf{H_t^{(o)^T}H_c^{(oo)}H_t^{(o)^T}H_c^{(oo)}}H_r^{(o)} + \left|H_t^{(l)}\right|^2 \left|H_c^{(lo)}\right|^2 H_r^{(o)} + \eta^{-1}H_r^{(o)} = T\mathbf{H_t^{(o)^T}H_c^{(oo)}} \quad \text{(A.43)}$$

$$\left|H_r^{(o)}\right|^2 \mathbf{H_c^{(oo)}H_c^{(oo)^T}H_t^{(o)}} + \beta\left|H_r^{(l)}\right|^2 \mathbf{H_c^{(ol)}H_c^{(ol)^T}H_t^{(o)}} + \boldsymbol{\lambda}\mathbf{H_t^{(o)}} = TH_r^{(o)}\mathbf{H_c^{(oo)}} \quad \text{(A.44)}$$

where

$$\eta = \frac{\sigma^2}{N_0 T} \quad \text{(A.45)}$$

Multiplying $(A.43)$ and $(A.44)$ by $H_r^{(o)}$ and $\mathbf{H_t^{(o)^T}}$ respectively

$$\left|H_r^{(o)}\right|^2 \mathbf{H_t^{(o)^T}H_c^{(oo)}H_t^{(o)^T}H_c^{(oo)}} + \left|H_r^{(o)}\right|^2 \left|H_t^{(l)}\right|^2 \left|H_c^{(lo)}\right|^2 + \eta^{-1}\left|H_r^{(o)}\right|^2 = T\mathbf{H_t^{(o)^T}H_c^{(oo)}}H_r^{(o)} \quad \text{(A.46)}$$

$$\left|H_r^{(o)}\right|^2 \mathbf{H_t^{(o)^T}H_c^{(oo)}H_c^{(oo)^T}H_t^{(o)}} + \beta\left|H_r^{(l)}\right|^2 \mathbf{H_t^{(o)^T}H_c^{(ol)}H_c^{(ol)^T}H_t^{(o)}} + \mathbf{H_t^{(o)^T}}\boldsymbol{\lambda}\mathbf{H_t^{(o)}} = T\mathbf{H_t^{(o)^T}H_c^{(oo)}}H_r^{(o)} \quad \text{(A.47)}$$

Equating $(A.46)$ and $(A.47)$ and recognizing that

$$\mathbf{H_t^{(o)^T}H_c^{(oo)}H_t^{(o)^T}H_c^{(oo)}} = \mathbf{H_t^{(o)^T}H_c^{(oo)}H_c^{(oo)^T}H_t^{(o)}} \quad \text{(A.48)}$$

we obtain

$$\mathbf{H_t^{(o)^T}}\left[\beta\left|H_r^{(l)}\right|^2 \mathbf{H_c^{(ol)}H_c^{(ol)^T}} + \boldsymbol{\lambda}\right]\mathbf{H_t^{(o)}} = \left|H_r^{(o)}\right|^2 \left[\left|H_t^{(l)}\right|^2 \left|H_c^{(lo)}\right|^2 + \eta^{-1}\mathbf{I}\right] \quad \text{(A.49)}$$

which leads to

$$\mathbf{H_t^{(o)^T}M_1H_t^{(o)}} = \left|H_r^{(o)}\right|^2 M_2 \quad \text{(A.50)}$$

where

$$\mathbf{M_1} = \beta\left|H_r^{(l)}\right|^2 \mathbf{H_c^{(ol)}H_c^{(ol)^T}} + \boldsymbol{\lambda} \quad \text{(A.51)}$$

$$M_2 = \left|H_t^{(l)}\right|^2 \left|H_c^{(lo)}\right|^2 + \eta^{-1} \quad \text{(A.52)}$$

Also, $(A.43)$ can be written as:

$$\mathbf{H_t^{(o)^T}H_c^{(oo)}H_c^{(oo)^T}H_t^{(o)}}H_r^{(o)} + \left|H_t^{(l)}\right|^2 \left|H_c^{(lo)}\right|^2 H_r^{(o)} + \eta^{-1}H_r^{(o)} = T\mathbf{H_t^{(o)^T}H_c^{(oo)}} \quad \text{(A.53)}$$

Substituting $(A.52)$ in $(A.53)$ and defining

$$\mathbf{M_3} = \mathbf{H_c^{(oo)}} \mathbf{H_c^{(oo)^T}} \tag{A.54}$$

leads to

$$\left[\mathbf{H_t^{(o)^T}} \mathbf{M_3} \mathbf{H_t^{(o)}} + M_2 \right] H_r^{(o)} = T \mathbf{H_t^{(o)^T}} \mathbf{H_c^{(oo)}} \tag{A.55}$$

Similarly substituting $(A.51)$ and $(A.54)$ in $(A.44)$ yields in

$$\left[\left| H_r^{(o)} \right|^2 \mathbf{M_3} + \mathbf{M_1} \right] \mathbf{H_t^{(o)}} = T H_r^{(o)} \mathbf{H_c^{(oo)}} \tag{A.56}$$

Vita

Monirosharieh Vameghestahbanati was born on June 17, 1987 in Iran. She was educated in local public schools and graduated from Dr. Hessabi High School, Shiraz, Iran, in 2005.

Ms. Vameghestahbanati moved to the United Arab Emirates with her family in 2005. She received her Bachelor of Science degree (summa cum laude) in Electrical Engineering from Ajman University of Science & Technology in 2010. She then joined the American University of Sharjah to pursue her M.S. degree, and granted the graduate teaching and research assistantship from there in 2010. She was awarded the Master of Science degree in Electrical Engineering in 2012.

Ms. Vameghestahbanati is a student member of IEEE, the Institute of Electrical and Electronics Engineers, got the first place in the fifth IEEE UAE student day common design project competition in May 2010, and has published a paper in the Wireless Telecommunications Symposium (WTS) in April 2012.